

Recent Progress on the Production of Aluminum Oxide (Al₂O₃) Nanoparticles: A Review

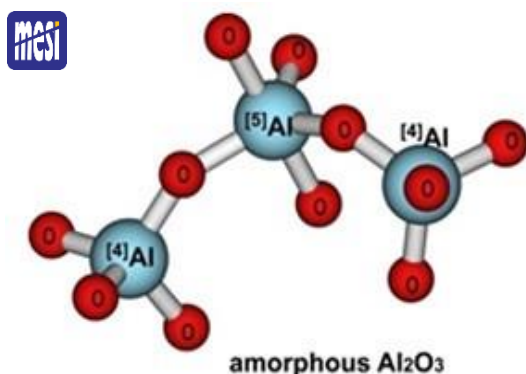
Adzra Zahra Ziva¹, Yuni Kartika Suryana¹, Yusrianti Sabrina Kurniadianti¹, Risti Ragadhita¹, Asep Bayu Dani Nandiyanto^{1*}, Tedi Kurniawan²

¹ Department of Chemistry, Faculty of Mathematics and Natural Sciences Education, Universitas Pendidikan Indonesia, Bandung 40154, **Indonesia**

² Engineering Technology Department, Community College of Qatar, Doha, **Qatar**

✉ nandiyanto@upi.edu

This article contributes to:



Highlights:

- Reviews on the production of aluminum oxide (Al₂O₃) was carried out
- Data obtained from research publications in 2004-2021
- Perspective advantages and disadvantages of the synthesis process have been reported
- Precipitation method is one of the best methods

Abstract

This study aims at discussing several methods to produce aluminum oxide (Al₂O₃) synthesis methods along with the advantages and disadvantages of each method used. In general, several methods are available: (1) precipitation, (2) combustion, (3) sol-gel, (4) wet chemical, (5) synthesis in supercritical water conditions, (6) microwave, (7) mechanochemical, and (8) hydrolysis, and the most efficient method for synthesizing Al₂O₃ is precipitation because it is facile and the simplest method (compared to other methods), can be proceeded using inexpensive raw materials, produces less pollution, and has several advantages: high purity product, high thermal stability, nearly homogeneous nanoparticle in size, and control desired particle size. The results of the study help to provide comparisons in producing various Al₂O₃ synthesis methods.

Keywords: Al₂O₃, Alumina, Aluminum oxide, Synthesis methods, Nanoparticles

Article info

Submitted:
2021-07-09

Revised:
2021-08-22

Accepted:
2021-08-28

Online first:
2021-09-08



This work is licensed under a Creative Commons Attribution-NonCommercial 4.0 International License

Publisher

Universitas Muhammadiyah
Magelang

1. Introduction

Nanoparticles or materials that are already small can cause physical and chemical properties to alter, resulting in new phenomena. Biomedical research, natural science, and science applications all benefit from nanoparticles. Drug transporters, cancer therapy, and cell imaging can all be done with nanoparticles [1,2]. In monolithic refractories, nanoparticles of α -Al₂O₃ with a narrow size demonstrate good flowability and can be used in radiators or sandpaper [3]. Aluminum oxide also can be used for microelectronic, catalysis, technical ceramics, and refractories [4]-[8].

Multi-phase nanoparticles are systems with diameters ranging from 1 to 100 nanometers. These materials have shown chemical, electrical, optical, mechanical, and magnetic properties that differ from bulk materials and their individual atomic constituents. Because nanoparticles have a larger surface area than micro and macroparticles, they are frequently used as adsorbents and catalysts [9,10].

Alumina is a chemical compound of aluminum oxide with the formula Al₂O₃. Alumina can be synthesized into several phases such as alpha, beta, gamma, and delta, with each phase reached at a different temperature during the synthesis process. Each phase has its properties with other uses. Alumina is often used in various applications because of its unique properties, such as

chemical and thermal stability, relative strength, good wear resistance, high hardness, high melting point, and good electrical and chemical resistance. This material can also act as a mediator in some chemical reactions [11,12].

In this article, we discuss the Al₂O₃ synthesis method. This article contains the methods and the advantages and disadvantages of Al₂O₃ synthesis. In this study, we found several ways to synthesize Al₂O₃ such as precipitation [13]-[26]; combustion [1], [27]-[30]; sol-gel [11,12], [30]-[37]; wet chemical [38]-[41]; synthesis water under supercritical water conditions [33]; microwave [44]; mechanochemical [41,44]; and hydrolysis [45]. Therefore, this paper aims to provide a review of what methods can be used and which method is more efficient in the Al₂O₃ synthesis process. It is hoped that this paper can positively affect the Al₂O₃ manufacturing industry in terms of production costs (economic evaluation), synthesis methods, and synthetic products.

2. Method

We conducted a literature review of several journals in 2004-2020. Several methods that can be used in the synthesis of Al₂O₃ can be seen in Table 1. It shows that Al₂O₃ can be synthesized through precipitation, combustion, sol-gel, wet chemical, supercritical water synthesis, microwave, and mechanochemical methods.

Table 1.
Methods, materials,
results, advantages,
disadvantages of the
synthesis of Al₂O₃

Method	Material	Result	Advantage	Disadvantage	Refs
Precipitation	Al(NO ₃) ₃ ·9H ₂ O, Na ₂ CO ₃ , and deionized water.	γ-Al ₂ O ₃ nanoparticles have a spherical shape, a size of 4.0-4.5 nm, a surface area of ~220 m ² /g, an average pore diameter of 7.0 nm, and a pore volume of ~0.487 cc/m ³ /g.	The synthesis method used is simple. The product has a high surface area, surface acidity, better crystallinity, and has high performance as a catalyst.	The synthesis process takes a long time.	[13]
	AlCl ₃ ·6H ₂ O, NH ₃ ·H ₂ O, and C ₂ H ₅ OH (95%).	γ-Al ₂ O ₃ nanoparticles are 5-9 nm in size and have a surface area of 204-102 m ² /g.	The synthesis process is low cost and without pollution.	The particles have heavy aggregation and the precipitate cannot be filtered easily.	[14]
	Al(NO ₃) ₃ ·9H ₂ O, Al ₂ (SO ₄) ₃ ·18H ₂ O, CO(NH ₂) ₂ , and aquades.	The diameters of α-Al ₂ O ₃ particles obtained from Al ³⁺ concentrations of 10 mmol/L and 0.5 mmol/L were 200-500 nm and 40-70 nm, respectively. The pore size of the α-Al ₂ O ₃ particles with a particle size of 40-70 nm, approximately 6-14 nm.	The synthesis method used is simple. The synthesized particles have high chemical stability, high thermal stability, and fine particle size.	A long time is required for the synthesis process.	[15]
	AlCl ₃ ·6H ₂ O, Al powder, HCl, and NH ₄ OH.	The Al ₂ O ₃ nanopowder has a size of 30-95 nm and is round in shape.	The synthesis method used is simple and the raw materials used are economical.	The synthesis process takes a long time.	[16]
	Al(N(CH ₃) ₂) ₃ and NH ₃ (25 wt %)	Pure γ-Al ₂ O ₃ nanopowder is 6-24 nm in size, has a surface area of 109-367 m ² /g, and has an almost spherical morphology.	The synthesis method used is simple and economical. The synthesized product has high quality/purity, as well as a high surface area.	The synthesis process takes a long time	[17]
	Sodium aluminate solution, HNO ₃ solution NH ₄ NO ₃ solution, and ethanol.	The average pore size is 12.9 nm, pore volume is 0.37 cm ³ /g, BET surface area is 86 m ² /g.	The synthesis method used is simple, and the cost of primary materials is cheap. Synthetic products with large surface area, large volume, good resistance, high purity and can be applied in the catalytic, adsorption, and separation fields.	The process of formation of the precipitate must be under the required pH.	[18]
	Al ₂ (SO ₄) ₃ ·18H ₂ O, Al(NO ₃) ₃ ·9H ₂ O, distilled water, polyethylene glycol 6000, and polyethylene glycol 200.	Nearly spherical γ-Al ₂ O ₃ nanoparticles with the ratio of n(SO ₄ ²⁻) to n(NO ₃ ⁻) are 2:8, 3:7, 4:6, and 5:5. The average particle size of γ-Al ₂ O ₃ is 23, 39, 5, 41.5, and 45 nm. Their particle size distributions are 11-37, 27-51, 27-60.5, and 29-61 nm, respectively.	This synthesis method can control the particle size to be produced.	A long time is required for the synthesis process.	[19]
	Al ₂ (SO ₄) ₃ ·18H ₂ O, water, NH ₃ ·H ₂ O (1,56 wt.%), and anhydrous ethanol.	Mesoporous Al ₂ O ₃ with surface area (412 m ² /g), pore volume (2.3 cm ³ /g), pore diameter (19.2 nm), and high thermal stability (up to 1000°C).	The synthesized product has high thermal stability and high surface area.	The synthesis process takes a long time	[20]

Method	Material	Result	Advantage	Disadvantage	Refs
	Al ₂ (SO ₄) ₃ ·18H ₂ O (99,9%), AlCl ₃ (99,9%), distilled water, urea (99%), tween80 (99%), sodium stearate (99,8%) surfactant, NaCl (99,9%), ethanol, and AgNO ₃ 0,1 M.	Al ₂ O ₃ particles with an average size of 0.4 m and round in shape. Particles with a spherical degree of 1.1 and a size of 0.36 micrometers were obtained when the optimum concentrations were 0.75 wt.% and 0.14 wt.%, respectively.	The method used is simple and has the potential to produce spherical ultrafine Al ₂ O ₃ particles that can be applied in the preparation of other spherical oxide powders.	The synthesis process takes a long time	[21]
	Al(NO ₃) ₃ ·9H ₂ O (95%), NH ₄ HCO ₃ (98%), deionization water, HNO ₃ , NaOH, ethanol, and acetone. Precipitating agent: Na ₂ CO ₃ (98%), NaHCO ₃ (99,5%), and (NH ₄) ₂ CO ₃ (99,9%).	γ-Al ₂ O ₃ powders which have a narrow size distribution of spherical nano-sized particles, with a surface area of ~140–190 γ-Al ₂ O ₃ , a crystal size of 4–6 nm, and a pore volume of 0.291–0.467 cm ³ g ⁻¹	γ-Al ₂ O ₃ powders have high purity.	A long time is required for the synthesis process.	[22]
	Sodium aluminate, carbon dioxide, oxalic acid, HG solid desilicizing agent, solid desodium agent I, and solid desodium agent II.	γ-Al ₂ O ₃ nanoparticles contain impurities, including iron, calcium, and silicon ions, with a low content of about 0.01%. γ-Al ₂ O ₃ nanoparticles have a large specific surface area and high pore volume of 269.9 m ² /g and 0.57 mL/g, respectively.	The synthesized product has high purity, high pore volume, and high specific surface area.	The synthesis process takes a long time. The synthesized product still contains impurities.	[23]
	NaOH, Al(NO ₃) ₃ , 5% Al(OH) ₃ bonded liquid, nano seed of α-Al ₂ O ₃ , 2% PEG20000, distilled water, ethanol.	α-Al ₂ O ₃ with a size of 30-40 nm.	The deposition process occurs very quickly, and the aggregation is reduced, resulting in much smaller particles.	It takes a long time to go through the synthesis process.	[24]
	AlCl ₃ ·6H ₂ O, liquid ammonia, ethanol (98%)	Most of the particles are in the range of 30-50 nm. The specific area of the gamma-alumina nanoparticles is 16.00 m ² /g and the maximum pore size is 4.13 nm.	The method used is easy, simple, and cost-effective. There is a weight loss of 4-6% at about 410 °C, and a total weight loss of only 23% when the temperature reaches 800°C.	The formation of a precipitate must be at the required pH level.	[25]
	AlCl ₃ ·6H ₂ O, polyvinylpyrrolidone (PVP)	The structure of α-Al ₂ O ₃ is rhombohedral. The average size of Al ₂ O ₃ nanoparticles is about 20 nm. Increasing the temperature causes the average particle size to decrease from 26 nm to 10 nm. Al ₂ O ₃ nanoparticles are spherical in shape and range in size from 20-50 nm.	The analysis was carried out without washing and purification.	PVP surfactants cause the nanoparticle size to decrease with increasing temperature.	[26]
Combustion	Solid rocket propellant containing 5-15 m aluminum, 200-400 m ammonium perchlorate, and binder.	Alumina nanoparticles are produced as aggregates consisting of primary particles. The diameter of the primary particles is in the range of 10-140 nm. The size of the aggregate varies in the range of 0.1 to several micrometers.	Combustion of solid propellants makes it easy to produce burnt aluminum droplets.	The average diameter of the particles varies greatly for different clusters.	[27]
	Extracted Al(OH) ₃ from local bauxite, and sugar.	Crystalline nanoparticles in the theta Al ₂ O ₃ phase. The average size is 15.5 nm. Al ₂ O ₃ spherical form with an average size of 30 nm.	The basic material for bauxite is found in Indonesia.	Although Al ₂ O ₃ nanoparticles were calcined at a relatively high temperature of 1200 °C, the particle size (15.5 nm) was still quite small.	[28]
	Al(NO ₃) ₃ ·9H ₂ O 99%, CO(NH ₂) ₂ 99%, nutrient media agar, ciprofloxacin, and double distilled water	The white solid is Al ₂ O ₃ , water (H ₂ O), nitrogen gas (N ₂), CO ₂ gas. The size of the nanoparticles is approximately 20 nm. The Eg value is about 5.25 eV. The area is 36 nm, the pore volume is 0.01 cm ³ , with a pore size of 1.3 nm.	Generates a more extensive area when using VCS mode.	The SCS method is a bit difficult because it will cause a precipitate when ammonium carbonate is added to ammonium nitrate.	[1]
	Al(NO ₃) ₃ ·9H ₂ O and (NH ₄) ₂ CO ₃	γ-alumina obtained has an area of about 300 m ² /g and a size of about 5 nm	Generates a more extensive area when using VCS mode.	The SCS method is a bit difficult because it will cause a precipitate when ammonium carbonate is added to ammonium nitrate.	[29]

Method	Material	Result	Advantage	Disadvantage	Refs
Sol-Gel	Aluminum isopro-poxide (99 wt%), 2-propanol, propionic acid, nitric acid (65 mass%), aluminum nitrat nonahydrate (98.5 wt%) potassium bicarbonate, distilled water.	γ -Al ₂ O ₃ nanoparticles with a surface area of 303 m ² /g, a pore volume of 0.55 cm ³ /g, a pore diameter of 7.4 nm, a crystal size of 4.7 nm, and a particle size of 4.9 nm.	The partial sintering particle size of the prepared sample is lower. The synthesized product has a high catalytic activity and better performance with the non-aqueous media sol-gel synthesis method.	The process of synthesizing is required a lot of time.	[30]
	Al(NO ₃) ₃ ·9H ₂ O, C ₆ H ₈ O ₇ ·H ₂ O, deionized water	γ -Al ₂ O ₃ measuring ~15 nm, which transformed into α -Al ₂ O ₃ with a size of 75 nm.	The method used is relatively simple, efficient, and cheap raw material	It takes a long time to go through the synthesis process.	[31]
	Aluminum iso-propoxide (AIP), 2-propanol (IPA) and acetic acid(AA), water.	γ -Al ₂ O ₃ nanoparticles with a surface area of 68.7 m ² /g, a pore volume of 0.62 cm ³ /g, and an average pore diameter of 34.7 nm.	The method used is simple. The product has a high surface area and high thermal stability.	The synthesis process takes a long time	[32]
	AlCl ₃ ·6H ₂ O, Al powder, HCl.	α -Al ₂ O ₃ nanoparticles with a size of 32-100 nm.	The method used is simple and the raw material is cheap. The product has high purity, it can be used as a starting powder for the fabrication of bulk alumina with nano microstructure.	The synthesis procedure is quite long.	[33]
	Aluminum chloride (AlCl ₃), ethyl alcohol (C ₂ H ₅ OH), and ammonium hydroxide (NH ₄ OH as 28% ammonia solution)	γ -Al ₂ O ₃ averaged about 30 nm for 0.1, 0.15, and 0.2 M AlCl ₃ , while the average was about 40 nm for 0.25 M AlCl ₃ .	Get a high yield of pure nano alumina particles. The results of the preparation of alumina particles are about 82-85%, the range of results is more satisfactory than the theoretical results.	The synthesis process takes a long time.	[34]
	Al(NO ₃) ₃ ·9H ₂ O, pure water, ethanol.	The nanoparticles have a polycrystalline structure and a rhombohedral structure. The average grain size of α -Al ₂ O ₃ is about 29 nm.	Simple and inexpensive. Does not require complicated tools for preparation.	Crystalline forms have heterogeneous sizes, different shapes, and spherical and semi-spherical shapes.	[12]
	Al(NO ₃) ₃ and (NH ₂) ₂ CO	Al ₂ O ₃ with a size of 4-400 nm. N ₂ , CO ₂ , and H ₂ O	Material which used not too much	The process takes a long time.	[35]
	AlCl ₃ , sucrose (C ₁₂ H ₂₂ O ₁₁), or starch (C ₆ H ₁₀ O ₅)	The area of Al ₂ O ₃ is 260,264 m ² /g. The average diameter is 6.26 nm.	Using organic ingredients (sucrose or starch).	The process takes a long time	[36]
	AlCl ₃ , 25%NH ₃ solution, and polyvinyl alcohol (PVA)	Aluminum oxide nanoparticles measuring 25 nm have a rhombohedral structure.	Quite affordable economically.	The process takes a long time	[37]
	Al(NO ₃) ₃ ·9H ₂ O, C ₆ H ₈ O ₇ ·H ₂ O, and deionized water	Amorphous structure at sintering temperatures of 600°C and 700°C. Sintering at 800°C changed the amorphous structure into γ -alumina crystals with an average crystal size of 11.5 nm. At 900°C, the average crystal growth reached 15.5 nm. At 1100°C and 1200°C, a white powder of α -alumina was formed with a crystal size of about 48 nm.	Precursors are used, which can control the stoichiometry and morphology of nanoparticles well. Provides high purity and high specific surface area of solid particles.	The process takes a long time	[11]
Wet Chemical	Aluminum nanoparticles with 99% purity, aluminum nitrate, distilled water, ammonia, dilute hydrochloric acid, ethanol	α -Al ₂ O ₃ like nanoplates with an average diameter of about 80 nm and a length of about 300–500 nm, without reaggregation.	This synthesis process can reduce the α -Al ₂ O ₃ phase formation temperature by about 200°C when compared to traditional wet chemical methods.	The synthesis procedure is quite long.	[38]
	Aluminum can, glacial acetic acid, HCl, NaOH, distilled water with electrical conductivity ~3 micro S/cm.	α -Al ₂ O ₃ nanoparticles with an average size of ~55 nm.	This method uses raw materials derived from recycling aluminum cans, which are economical and can reduce waste.	The process takes a long time for the synthesis of aluminum acetate precursors.	[38]
	Commercial Al nanometer powder (particle size 80–100 nm, 99% purity), aluminum nitrate (99% purity), HCl, ethanol, and ammonia.	α -Al ₂ O ₃ nanoparticles with an average size of 10–20 nm and resulted in a well-dispersed alumina-coated Al composite with a spherical shape.	A fine transition layer is formed between Al and Al ₂ O ₃ , which can increase the bond between Al and Al ₂ O ₃ . This method is suitable for the synthesis of composite ceramics. Al ₂ O ₃ - Al.	A long time is required for the synthesis process.	[40]

Method	Material	Result	Advantage	Disadvantage	Refs
	AlCl ₃ .6H ₂ O and NH ₄ HCO ₂ . Soluble starch, deionized water, and ammonium hydroxide.	AACH, which transforms into the α-Al ₂ O ₃ at temperatures of 1150-1100°C, is 20-30 nm in size.	Adding AlCl ₃ solution at a rate of less or more than 1.2 L/h will produce AACH and γ-AlOOH so that it will still produce α-Al ₂ O ₃ .	The process is quite long, and the nanoparticles that accumulate are quite a lot.	[41]
Synthesis under supercritical water conditions	Al(NO ₃) ₃ .9H ₂ O 99%, and distilled water 18 ohm.	The products are γ-Al ₂ O ₃ , HNO ₃ , H ₂ O, and γ-AlOOH.	The temperature used is relatively low compared to other methods, and the results obtained are pretty small.	Still need further experiment for dispersing agent	[42]
Microwave	Aluminum Nitrate (>98%), plant extracts (Syzygium aromaticum, Origanum vulgare, Origanum majorana, Theobroma cacao, and Cichorium intybus), ethanol	All nanoparticles appear to have a nearly spherical shape. The nanoparticle clusters are between 60-300 nm.	Microwave radiation can be used as a powerful heat source for the synthesis of nanoparticles from the liquid phase in a short time.	The nanoparticles are significantly smaller than the dimensions estimated from the SEM images, which may be rooted in the agglomeration of the nanoparticles.	[43]
Mechano-chemical	AlCl ₃ .6H ₂ O and NH ₄ HCO ₃ . Soluble starch, deionized water, and ammonium hydroxide.	AACH, which transforms into α-Al ₂ O ₃ at the temperature of 1150-1100°C, is 30-40 nm in size.	Compared with the wet chemical method, this method is simpler, the calcination temperature is lower, and the resulting nanoparticles are less agglomerated, making them more suitable for commercial manufacture.	The pH must be maintained at 9-10 by adding ammonium hydroxide.	[41]
	Fe ₂ O ₃ and Al	Al ₂ O ₃ with a size of 12 nm and Fe	This mechanochemical method requires low manufacturing costs for large quantities	The pH must be maintained at 9-10 by adding ammonium hydroxide.	[44]
Hydrolysis	Aluminum phosphide powder (>85%), deionized water.	γ-Al ₂ O ₃ nanoparticles with a surface area of 285 m ² /g.	The synthesized product has high thermal stability.	A long time is required for the synthesis process.	[45]

3. Results and Discussion

Based on the reviewed studies, several general methods for synthesizing Al₂O₃ include precipitation, combustion, sol-gel, wet chemical, supercritical water synthesis, microwave, mechanochemical, and hydrolysis. The methods and results of several studies will be discussed below.

3.1. Precipitation method

Precipitation is the most common method for the synthesis of Al₂O₃ nanoparticles because this method is the simplest [13]-[23], low raw material cost [16]-[18], and without pollution [14]. The precipitation method has several advantages, such as high purity products [17], [18], [22], [23], high thermal stability [15,20], nearly homogeneous nanoparticles in size [25], and control the desired particle size [19]. The precipitation method forms a solution as a phase transition of alumina [17]. The pH and temperature of the solution in the formation process are critical for this method.

The starting materials used in this method are Al(NO₃)₃.9H₂O, Al(NO₃)₃.9H₂O, CO(NH₂)₂, anhydrous alcohol, and distilled water. These ingredients are weighed and measured in stoichiometric ratios. The solution was made by dissolving the reagents Al(NO₃)₃.9H₂O and Al₂(SO₄)₃.18H₂O into distilled water. After that, CO(NH₂)₂ is added to the solution, and the solution mixture is heated to 95°C. Then, the resulting Al(OH)₃ precipitate was washed and dried at 60°C. After that, the product was calcined for 2 hours and cooled at room temperature [15].

The synthesis results showed that the Al(OH)₃ particles formed from the aggregation of small primary colloids would experience particle shrinkage, increasing pore size during the calcination process. X-ray diffraction (XRD) using an X-ray diffractometer (Rigaku D/max-2400, Japan) with Cu K_α radiation (40 kV, 60 mA) in the 2θ range of 10°–80° was used to study the crystal structures of the samples. The measurement was carried out at a 5°/min scan rate with a 0.02° step size. Based on XRD analysis, during the calcination process of Al(OH)₃ particles, a phase transformation occurred with the amorphous sequence Al(OH)₃ → γ-Al₂O₃ → α-Al₂O₃. Figure 1 presented the X-ray Diffraction (XRD) pattern of Al(OH)₃ particles calcined at different temperatures for 2 hours. A field-

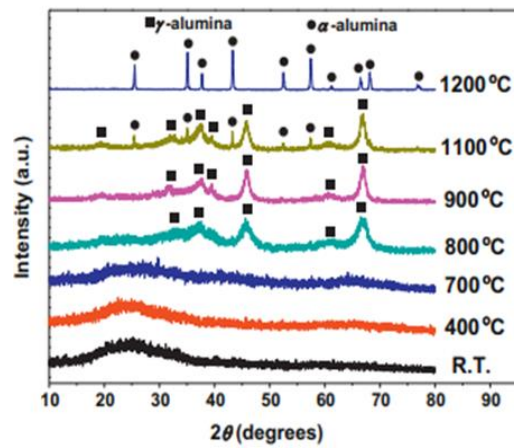


Figure 1.
XRD pattern of sample
calcined results [15]

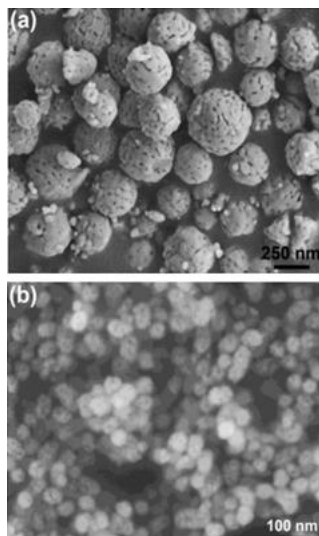


Figure 2.
SEM micrograph of α - Al_2O_3 particles with
 Al_3^+ concentration (a) 10
mmol/L and (b) 0.5
mmol/L [15]

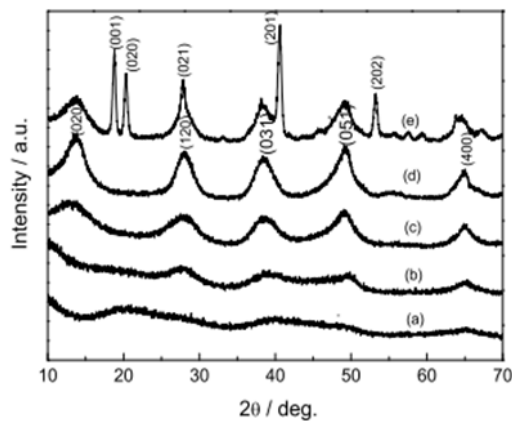


Figure 3.
XRD pattern of
precipitates at various pH
levels: a) pH=5, b) pH=6,
c) pH=8, d) pH=10, and e)
pH=11 [18]

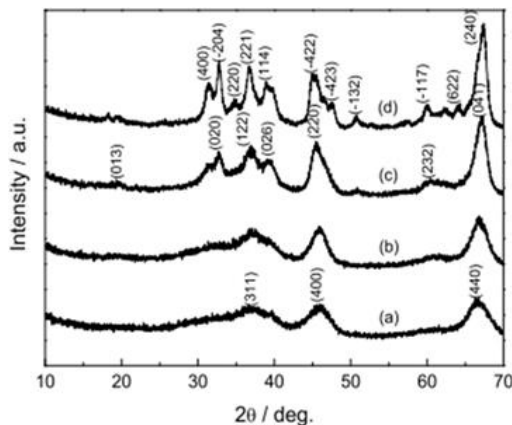


Figure 4.
XRD pattern of calcined
precipitate at (a) 500°C,
(b) 700°C, (c) 900°C, and
(d) 1000°C temperatures
[18]

emission scanning electron microscope (SEM, Hitachi S-4800, Tokyo, Japan) was used to investigate the morphologies of the samples at a voltage of 15 kV. The SEM analysis shows the particles have monodisperse and spherical shapes. **Figure 2** shows an SEM micrograph of α - Al_2O_3 particles obtained from calcining $\text{Al}(\text{OH})_3$ at 1200°C for 2 hours. The diameters of α - Al_2O_3 particles obtained from Al^{3+} concentrations of 10 mmol/L and 0.5 mmol/L were 200-500 nm and 40-70 nm, respectively. The diameter of these particles can be changed by adjusting the concentration of Al^{3+} in the solution. The higher the Al^{3+} concentration shows the larger particle diameter [15].

This synthesis uses starting materials, namely sodium aluminate solution, HNO_3 solution, NH_4NO_3 solution, and ethanol. These ingredients are weighed and measured in stoichiometric ratios. The sodium aluminate solution is pumped into the HNO_3 solution at 30°C. Then, the white precipitate was covered (sealed with PE film), reacted at 30°C, and ripened at 60°C. After ripened, the colloid was filtered and washed with a solution of NH_4NO_3 and ethanol. Afterward, the colloid was dried at 110°C, calcined to 500°C, and heated at 500°C for 4 hours [18].

XRD pattern of dry boehmite samples obtained at various pH levels is shown in **Figure 3**. A pure crystalline boehmite phase with an orthorhombic structure was formed when the basicity of the reaction solution was elevated to pH=10, and no impurity peaks were observed, indicating a high purity product. The condition of pH=10 and an aging time of 10 hours were chosen as the optimal synthesis conditions. **Figure 4** shows the XRD pattern of alumina samples calcined at various temperatures. The diffraction pattern of the boehmite phase was changed into the γ - Al_2O_3 phase with cubic symmetry at a calcination temperature of 500°C. No significant changes were found in the structure after heat treatment increased to 700°C. Increasing the calcination temperature up to 900°C displays a new phase transformation, namely δ - Al_2O_3 . The formation of the θ - Al_2O_3 phase with monoclinic symmetry at a calcination temperature of 1000°C was confirmed by fourier transform infrared (FTIR) measurements. The SEM micrographs of γ - Al_2O_3 particles calcined at 500°C with a size of 200-100 nm and θ - Al_2O_3 particles calcined at 1000°C with a size of 100 nm were shown in **Figure 5** [18].

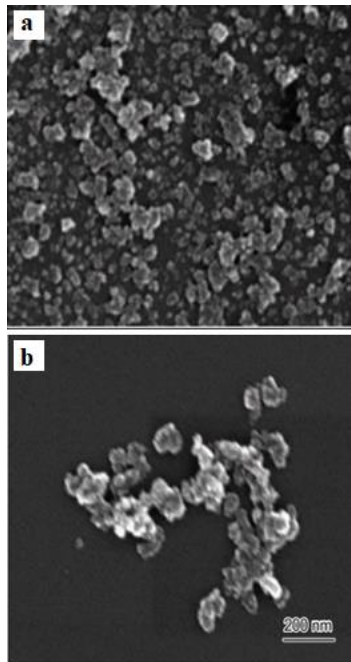


Figure 5.
SEM of alumina powder after being calcined at: a) 500°C and b) 1000°C [18]

Gamma-alumina nanoparticles synthesized through the method of precipitation in water. $\text{AlCl}_3 \cdot 6\text{H}_2\text{O}$ was dissolved in deionized water and Tween-80 (polyoxyethylene sorbitan monooleate) was added to the solution as a surfactant. Then, as a precipitating agent, a solution of formamide in water is added dropwise to the mixture. The presence of a white gelatin precipitate shows that $\text{Al}(\text{OH})_3$ has formed. This precipitate was filtered and washed numerous times with ethanol and water. After drying, the white gel was calcined for 5 hours in the air in a muffle furnace at 550°C, converting $\text{Al}(\text{OH})_3$ into Al_2O_3 nanoparticles. These ingredients are weighed and measured in stoichiometric ratios [25].

The formation of alumina nanoparticles occurs in 2 stages, the nucleation stage, and the formation of nanoparticles. Tween-80 is dispersed in water as a spherical nuclear-shell micellar structure with a core of C-C hydrophobic chains and a shell of polar $-\text{OH}$ groups. Formamide (HCONH_2) plays an important role in the formation of nanoparticles by decomposing to produce OH^- ions in water which react with Al^{3+} ions to form $\text{Al}(\text{OH})_3$ and precipitation occur after the pH value of the solution reaches the required level. Alumina nanoparticles are formed when $\text{Al}(\text{OH})_3$ is calcined in an inert environment. The schematic of the synthesis of Al_2O_3 nanoparticles is shown in Figure 6 [25].

Ali *et al.* [25] reported nanoparticle morphology determined by SEM and Transmission electron microscopy (TEM) analysis (Figure 7 and Figure 8). The majority of the particles were in the 30-50 nm range, according to scanning electron microscopy (SEM) analysis. The size distribution also confirms that most of the nanoparticles are nearly homogeneous in size and proportions. The energy dispersive X-ray (EDX) element mapping (Figure 9) shows the aromatic structure. These compounds show great resistance to heat and light, so their degradation requires severe conditions. According to the Brunauer–Emmett–Teller (BET) method, the gamma-alumina nanoparticles had a specific area of 16.00 m^2/g and a maximum pore size of 4.13 nm.

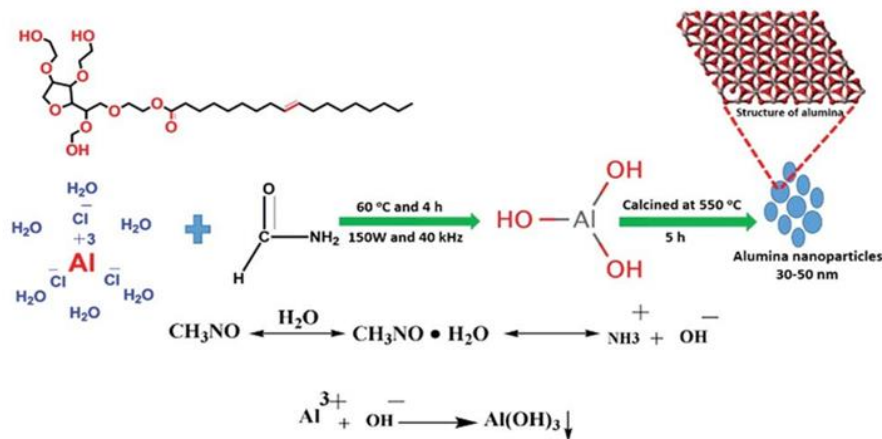


Figure 6.
Schematic synthesis of alumina nanoparticle formation [25]

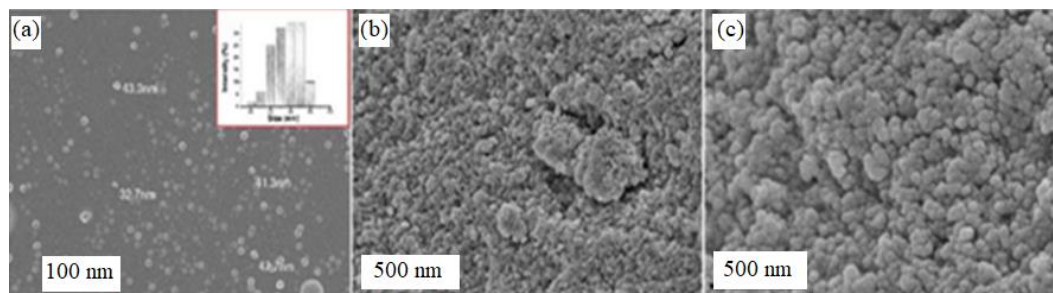


Figure 7.
SEM images of nanoparticles: (a) in the presence of Tween-80 and formamide, (b) without Tween-80, and (c) without formamide. The inset in (A) depicts the size distribution of the nanoparticles [25]

Figure 8.
TEM images of nanoparticles: (a) in the presence of Tween-80 and formamide, (b) without Tween-80, and (c) without formamide [25]

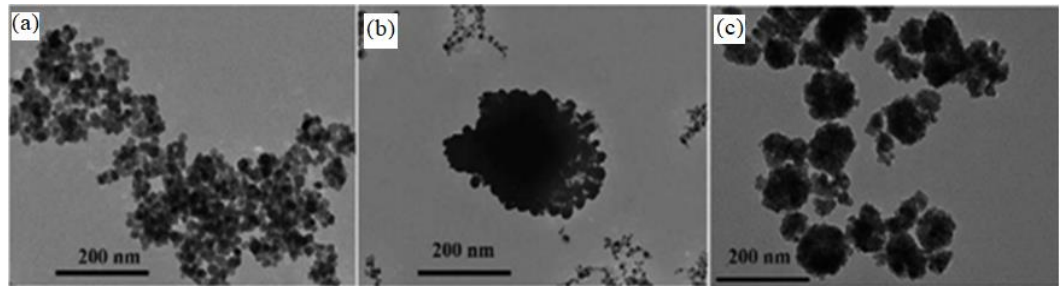
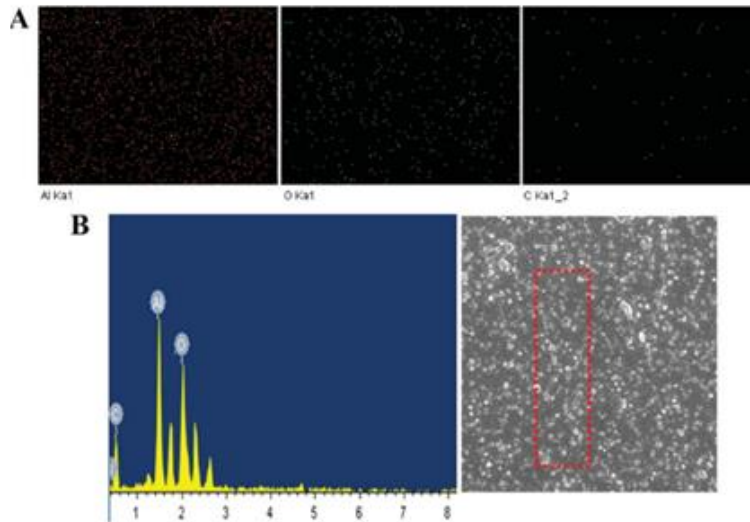


Figure 9.
(A) Mapping of EDX elements and (B) EDX spectra of nanoparticles [25]



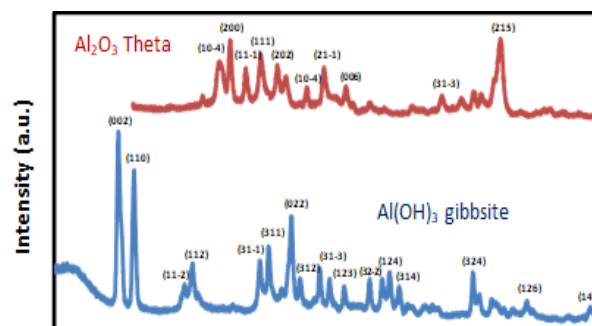
3.2. Combustion method

The SCS (Solution Combustion Synthesis) process is a self-contained chemical complex that requires a homogeneous precursor solution. SCS begins with the dehydration and decomposition of a homogeneous solution and involves many exothermic reactions that produce at least one solid and a considerable volume of gas [46]. Kandil *et al.* [47] stated that this method is inexpensive, convenient, and economical.

Syarif *et al.* [28] synthesize Al_2O_3 nanoparticles using the self-combustion method from bauxite using sugar as fuel. $\text{Al}(\text{OH})_3$ is extracted from local bauxite. $\text{Al}(\text{OH})_3$ powder is put into a beaker filled with water. Pour some sugar into a beaker until it is completely dissolved. The mixture forms a sol. The ratio of $\text{Al}(\text{OH})_3$ with sugar is 1:1. To make a gel, the sol is heated to 150°C . The gel self-combusted at 450°C and was heated for 10 minutes at 600°C . After that, the material was calcined for an hour at 1200°C to form Al_2O_3 nanoparticles.

The results of the synthesis of Al_2O_3 Syarif *et al.* [28] show crystal nanoparticles in the theta Al_2O_3 phase. This shows the role of sugar in inhibiting the formation of the alpha phase during calcination. The sugar utilized binds Al ions, requiring a calcination temperature of more than 1200°C and a period of more than 1 hour to generate the alpha-alumina phase. According to the Debye Scherrer method of XRD pattern calculation, the average size is 15.5 nm (Figure 10). Although Al_2O_3 nanoparticles were calcined at a relatively high temperature of 1200°C , the particle size (15.5 nm) was still quite small. The TEM image shows the spherical shape of Al_2O_3 with an average size of 30 nm (Figure 11).

Figure 10.
XRD pattern of $\text{Al}(\text{OH})_3$ extract from local bauxite and Al_2O_3 nanoparticles synthesized using self-combustion with sugar as fuel calcined at 1200°C for 1 hour [28]



Afruz & Tafreshi [29] synthesized $\gamma\text{-Al}_2\text{O}_3$ nanoparticles using the combustion method and ammonium carbonate catalyst. The combustion methods used are solid-state combustion (SSC) and solution combustion state (SCS). The materials used in all types of combustion are $\text{Al}(\text{NO})_3 \cdot 9\text{H}_2\text{O}$ and $(\text{NH}_4)_2\text{CO}_3$. So, expect a reaction is presented in Equation (1).

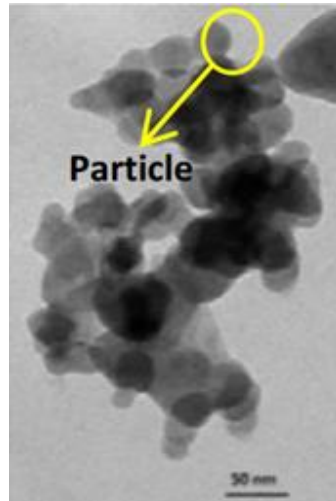
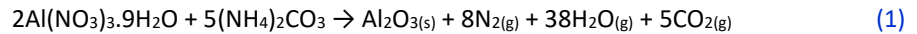


Figure 11. TEM image of Al_2O_3 nanoparticles. The average particle size is 30 nm [28]

The solid-state combustion method is carried out using the volume combustion synthesis (VCS) mode. It can produce nano size with a high area and requires a weak exothermic reaction that requires activation by pre-heating or an electric field. This method is done by mixing the ingredients by grinding in a mortar, and then it will form water, emit CO_2 , and dry quickly [29].

Solution combustion synthesis (SCS) is a process that combines combustion with the solution. An exothermic chemical reaction between the salt and the required metal and organic fuel is used in this approach. When ammonium carbonate is added to aluminum nitrate, a precipitate forms, this procedure is complicated. As a result, this procedure is split into two parts: gel combustion synthesis and traditional VSC [29].

Different results are produced due to the comparison of various combustion modes by Afruz & Tafreshi [29]. The XRD pattern shows that the same sample has an incomplete structure in sample d-1 compared to other samples (Figure 12). Alumina has an area above $300\text{--}400 \text{ m}^2/\text{g}$, but the pore size is often wide, even bimodal (Figure 13), and the fine crystal size is about 5 nm (Figure 14 and Figure 15). This experiment shows that using VCS mode in SCS to synthesize Al_2O_3 nanoparticles can produce a higher and specific area than solid combustion.

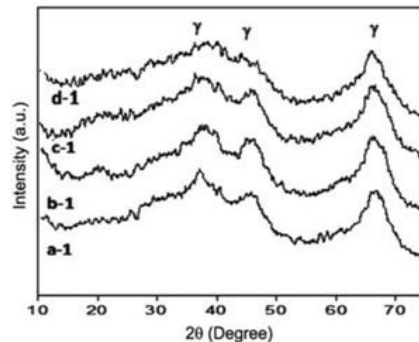


Figure 12. TEM image of Al_2O_3 nanoparticles. The average XRD pattern on synthetic powders prepared by different combustion modes [29]

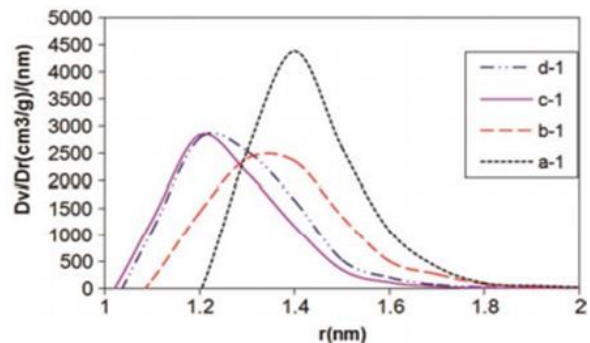


Figure 13. Distribution of the pore sizes in the synthesized powder from the MP Plot [29]

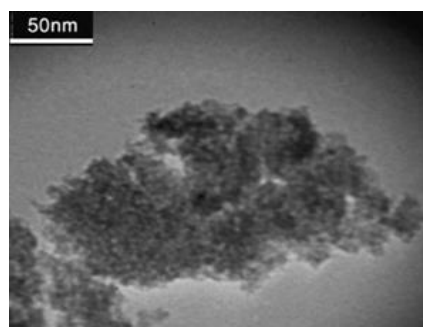


Figure 14. TEM of one of the samples [29]

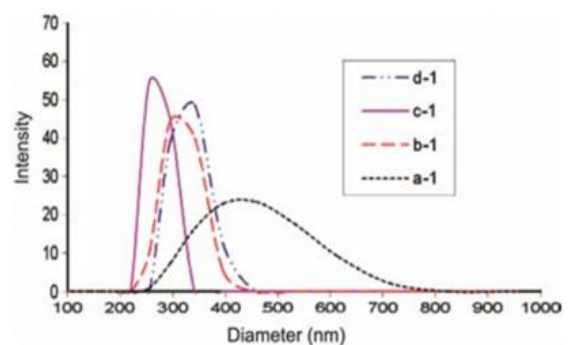


Figure 15. Particle size distribution and synthetic powder [29]

3.3. Sol-Gel method

The sol-gel method is a simple and effective method for synthesizing Al_2O_3 nanoparticles. The most obviously difference in this method compared to the precipitation method is that the precipitate is converted into a sol and a gel first. Low synthesis temperature [30],[31],[48]; low raw material cost [31],[33]; high thermal stability [32]; high purity [48]; and high surface area [32] are some of the benefits of the sol-gel method.

The raw materials for this synthesis are $\text{Al}(\text{NO}_3)_3$ and $\text{C}_6\text{H}_8\text{O}_7 \cdot \text{H}_2\text{O}$. The stoichiometric ratios of these ingredients are weighed and measured. Aluminum nitrate and citric acid were dissolved in deionized water at 60°C until a yellowish sol formed. Next, the yellowish sol is heated to 80°C —

the viscosity and color of the sol change to a transparent gel. The gel was heated at 200°C, ground to a fine powder, and calcined [31].

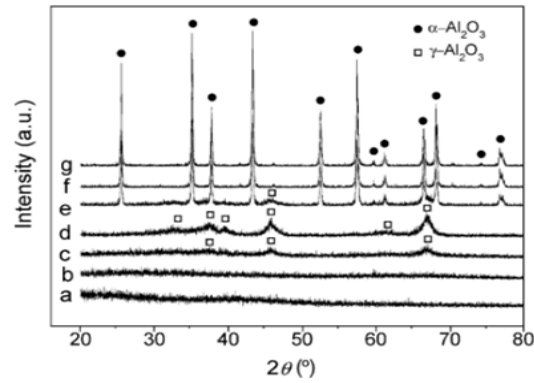


Figure 16. XRD pattern of the synthesized precursor (C/N = 1) calcined at different temperatures (a) 200°C, (b) 600°C, (c) 800°C, (d) 900°C, (e) 950°C, (f) 1000°C, and (g) 1100°C [31]

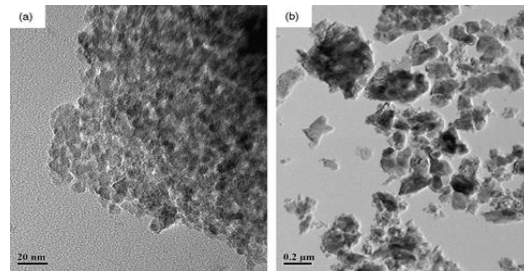


Figure 17. FETEM micrograph of the synthesized precursor (C/N = 1) calcined at (a) 950°C and (b) 1000°C [31]

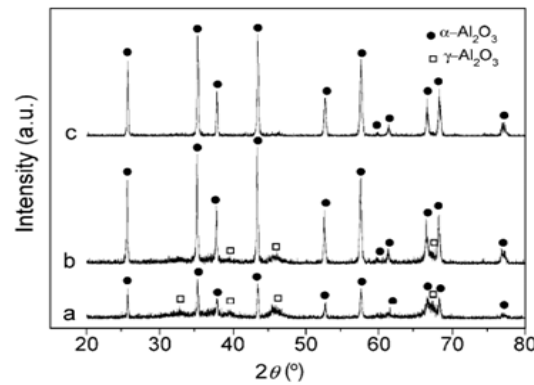


Figure 18. XRD pattern of α -Al₂O₃ calcined at 1000°C (a) C/N = 0.5; (b) C/N = 1.0; and (c) C/N = 2.0 [31]

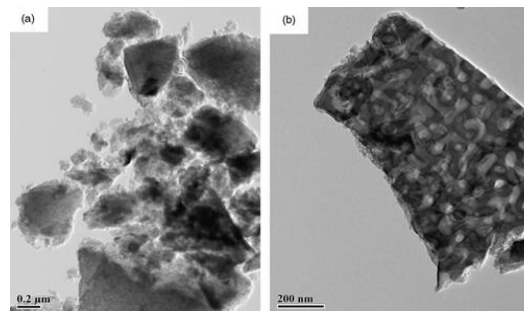


Figure 19. FETEM micrograph of α -Al₂O₃ calcined at 1000°C (a) C/N = 0.5 and (b) C/N = 2.0 [31]

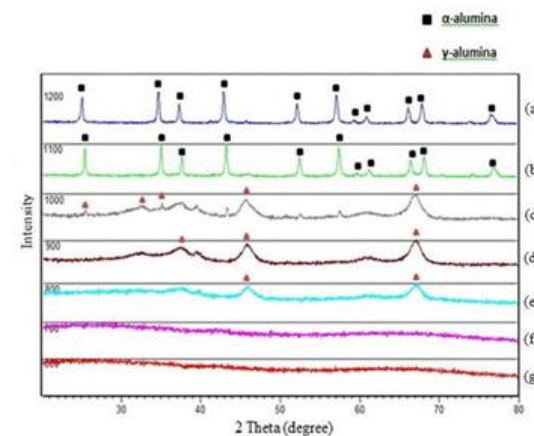


Figure 20. XRD pattern of synthesized and heat-treated samples at: (a) 1200°C, (b) 1100°C, (c) 1000°C, (d) 900°C, (e) 800°C, (f) 700°C, and (g) 600°C [11]

The XRD analysis was used to identify the nanoparticle phase produced during the synthesis. The XRD pattern of the synthesized powder with a C/N ratio of 1.0, which was calcined at various temperatures, is shown in Figure 16. The characteristic low-intensity γ -Al₂O₃ peak was reached at 800°C, indicating the transition from the amorphous phase to γ -Al₂O₃. At 950°C, a weak peak of α -Al₂O₃ was seen, indicating the transition from the γ - to α -Al₂O₃ phase. Figure 17 reveals a field emission transmission electron microscope (FETEM) micrograph with a citrate precursor ratio of C/N = 1.0. The amount of α -Al₂O₃ increased dramatically when the calcination temperature was above 1000°C. The XRD pattern of powders obtained from various precursor ratios and calcined at 1000°C is shown in Figure 18. The α -Al₂O₃ XRD pattern profile became sharper as the C/N mole ratio increased, with the characteristic peak of γ -Al₂O₃ weakening and disappearing. Figure 19 shows the SEM micrograph created at 1000°C calcination. The calcined Al₂O₃ powder from C/N = 0.5 shows many plate-like flake structures and mixed multi-modal crystallites in Figure 19(a). Meanwhile, as shown in Figure 19(b), the mole ratio of C/N = 2.0 exhibits severe agglomeration. The molar ratio of C/N = 1 yielded relatively good results with α -Al₂O₃ ultrafine powder with a particle size of 200 nm, according to the results of the study [31].

Mohamad *et al.* [11] synthesized alumina nanoparticles by sol-gel method using aluminum nitrate ((Al(NO₃)₃·9H₂O), citric acid (C₆H₈O₇·H₂O), and deionized water. These materials were weighed and measured in stoichiometric ratios. Aluminum nitrate was dissolved with citric acid in deionized water. The solution was stirred at 60°C until it turned into a yellowish sol. The solution was then heated to 80°C and stirred constantly until a transparent gel was formed. In an oven, the gel was dried at 90°C. The dry gel was ground and sintered at various temperatures, such as 600°C, 700°C, 800°C, 900°C, 1000°C, 1100°C, and 1200°C.

The results of the synthesis showed that only samples were sintered at temperatures of 1000°C, 1100°C, and 1200°C which turned into a white powder. Sintering at temperatures below 1000°C produces a black powder. The residual carbon inherited from the sol that is not completely burnt is assumed to be responsible for the appearance of black powder. The amorphous

structure obtained for the powders sintered at 600°C and 700°C can be seen in the XRD pattern (Figure 20). When the sintering temperature was increased to 800°C, it showed a transition from the amorphous structure to the γ -alumina phase. At 900°C, the production of γ -alumina becomes more intense. Alumina begins to grow when the temperature reaches 1000°C. At 1100°C, the transition from γ -alumina to α -alumina is complete. The α -alumina phase does not change at a sintering temperature of 1200°C. At sintering temperatures of 600°C and 700°C, due to the amorphous structure, no crystal size can be determined. The average crystal size for those sintered at 800°C is 11.5 nm. When the temperature was increased to 900°C, the average crystal growth reached 15.5 nm and this value was not much different from that of the sample sintered at 1000°C consisting of a mixed alumina phase. Significant crystal growth was seen when the sintering temperature was increased to 1100°C and 1200°C where the average crystal sizes were 46.6 nm and 49.1 nm, respectively. Figure 21 shows the SEM micrograph of the nanoparticles [11].

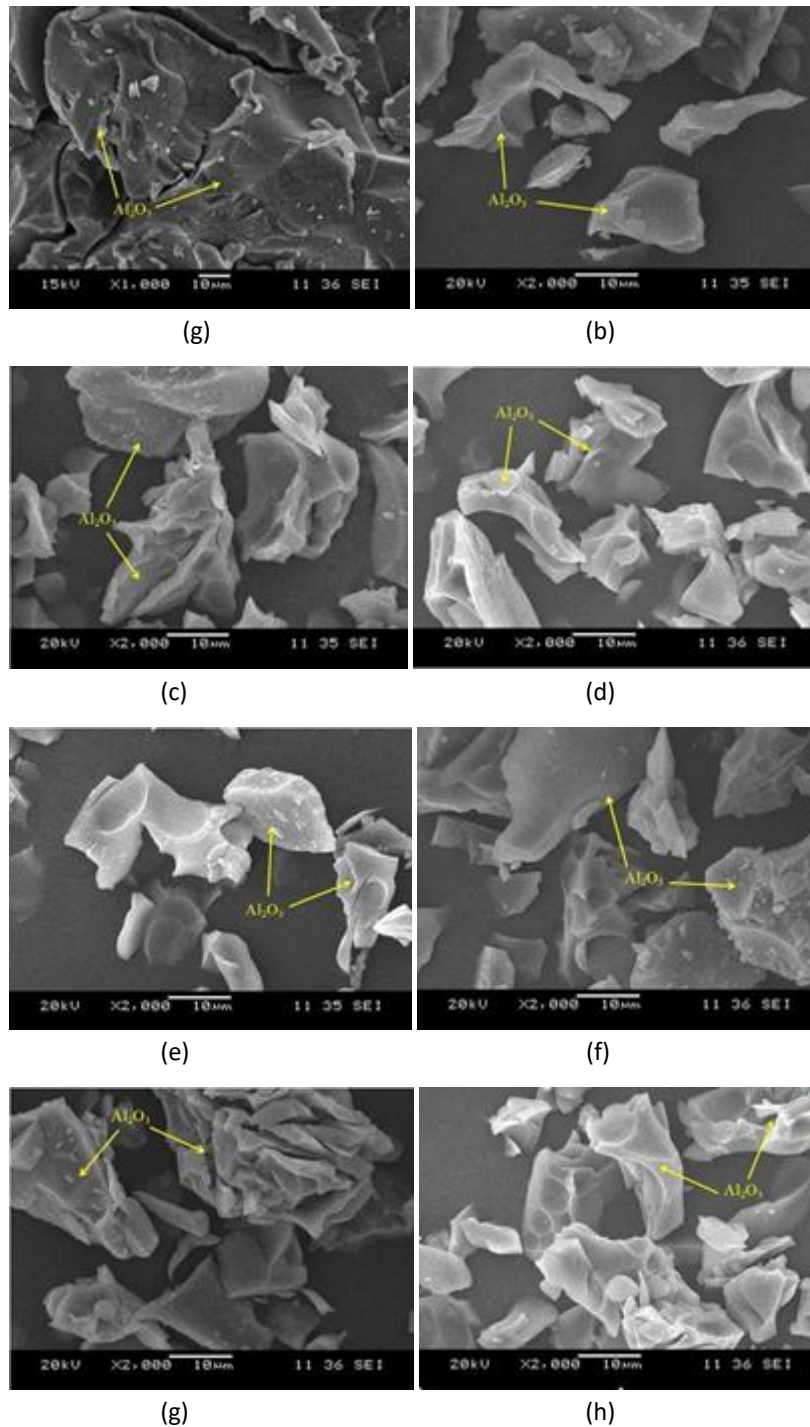


Figure 21. SEM micrograph of alumina nanoparticles sintered at different temperatures: (a) 0°C, (b) 600°C, (c) 700°C, (d) 800°C, (e) 900°C, (f) 1000°C, (g) 1100°C, and (h) 1200°C [11]

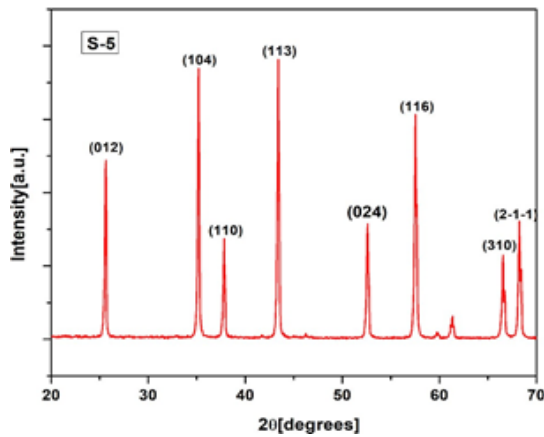


Figure 22.
Micrograph XRD of nanoparticles prepared by the SGAC method [35]

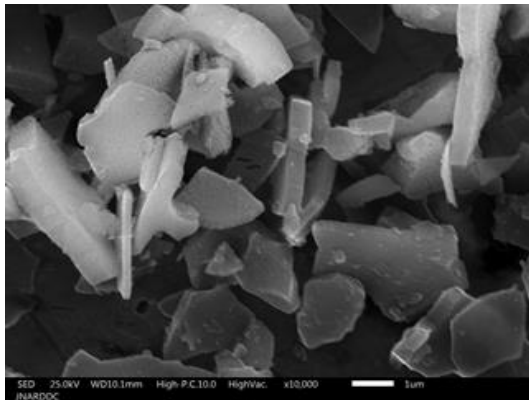


Figure 23.
SEM micrograph of nanoparticles using the SGAC method [35]

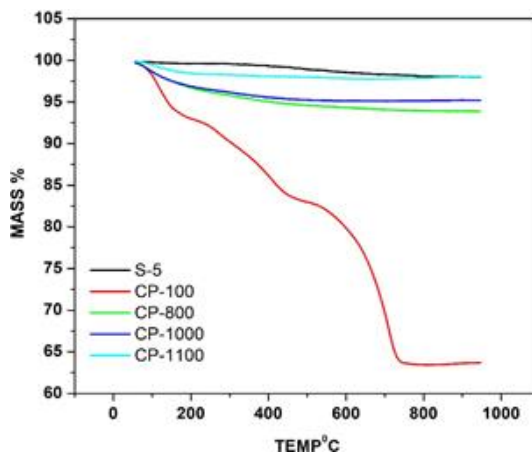
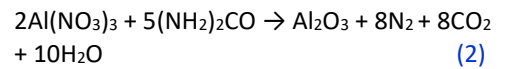


Figure 24.
TGA of alumina powder prepared by chemical precipitation (CP) and sol-gel auto combustion techniques (S-5) [35]

Nayar *et al.* [35] used aluminum nitrate ($\text{Al}(\text{NO}_3)_3$) and urea ($(\text{NH}_2)_2\text{CO}$) to make Al_2O_3 nanoparticles. Aluminum nitrate and urea are dissolved in distilled water to make sol. This sol is heated to 70–80°C in a stirring position on a hot plate for 4–5 hours, yielding a translucent and colorless gel. At a specific time, the gel is immersed in a bath with a temperature of 450–600°C. As a result, the reaction's formula is presented in Equation (2).



The results obtained by Nayar *et al.* [35] is a crystal size 44.42 nm. The regular decomposition of aluminum nitrate and urea helps obtain alpha-alumina nanoparticles at a relatively low temperature compared to the non-fuel synthesis, periodically converted to alpha at 1100°C.

Figure 22 presented the XRD diffractogram for the nanoparticles. Samples that are heated at high temperatures have the same XRD pattern as alpha-alumina in the irreversible phase. Figure 23 shows the SEM image of the alumina morphology with the calcination temperature increasing from 800 to 1100°C. Figure 24 depicts the thermogravimetric Analysis (TGA) of all samples and their mass loss comparisons based on increasing temperature.

3.4. Wet chemical method

The Al_2O_3 nanoparticles were successfully synthesized by the wet chemical method. In this method, the precipitate formed is obtained by dropping the precipitate into the solution at a specific rate. The pH of the solution strongly influences this method. The wet chemical has several advantages, including raw materials derived from waste recycling [38], the resulting product has a uniform size and high thermal stability [39].

Aluminum nanoparticles (100 nm) with 99% purity, aluminum nitrate, distilled water, ammonia, dilute hydrochloric acid, and ethanol are used as starting materials in this method. The synthesis process is depicted in Figure 25 in the flow diagram. In stoichiometric ratios, these materials are weighed and measured. First, distilled water is used to dissolve aluminum nitrate. Then, aluminum nanopowder was added, and ammonia was dripped into the mixture at a speed of 100 drops/minute. To prevent aggregation, dilute hydrochloric acid is added. The pH value of the solutions was maintained at 6, throughout the reaction. The composite deposit was filtered and washed with distilled water or ethanol. Next, the precipitate obtained was dried at 80°C and calcined to 1100°C [38].

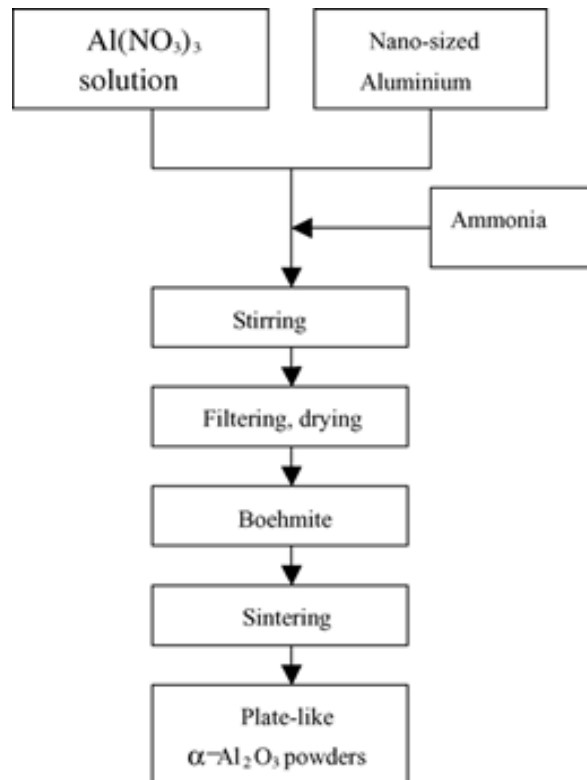


Figure 25.
Flowchart of the synthesis procedure [38]

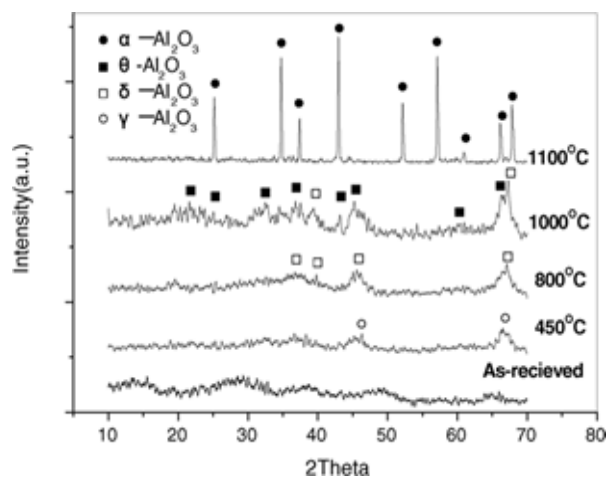


Figure 26.
XRD pattern: (a) dry gel, (b) sintered at 500°C, (c) sintered at 800°C, and (d) sintered at 1100°C [38]

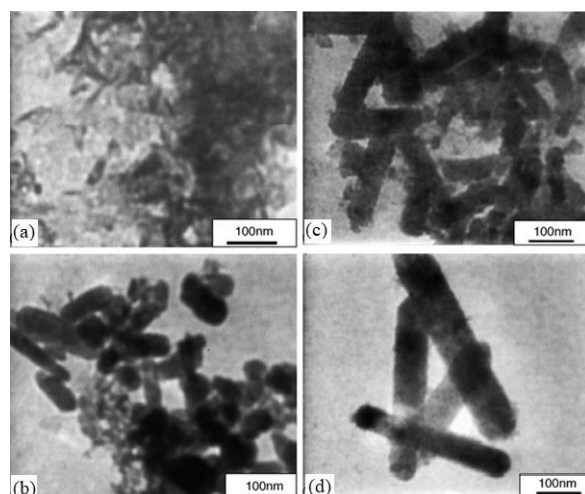
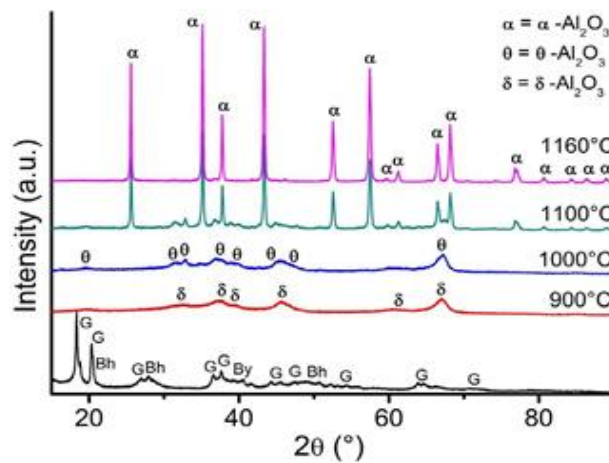


Figure 27.
TEM micrograph of sintered boehmite at different temperatures: (a) dry gel, (b) 500°C, (c) 800°C, and (d) 1100°C [38]

The precursor phase before and after calcination was determined by XRD analysis. Figure 26 presented the synthesized XRD pattern with different calcination temperatures. The γ - Al_2O_3 phase was observed after the sample was calcined at 450°C. Only the δ - Al_2O_3 phase was observed at a calcination temperature of 800°C. When the temperature is raised to 1000°C, the θ - Al_2O_3 phase takes over, and when the temperature is raised to 1100°C, the complete α - Al_2O_3 phase is obtained. Compared to the traditional wet chemical method, the addition of aluminum additives reduced the α - Al_2O_3 phase formation temperature by about 200°C. The powder shape and particle size of the synthesized product were observed by TEM, as shown in Figure 27. The TEM observations verified that the dried boehmite particles looked like fibers (Figure 27a). Increasing calcination temperature causes an increase in particle size, and its shape becomes like a plate. These plate-like Al_2O_3 grains have a mean diameter of about 80 nm and a length of about 300-500 nm, without reaggregation, as shown in Figure 27d [38].

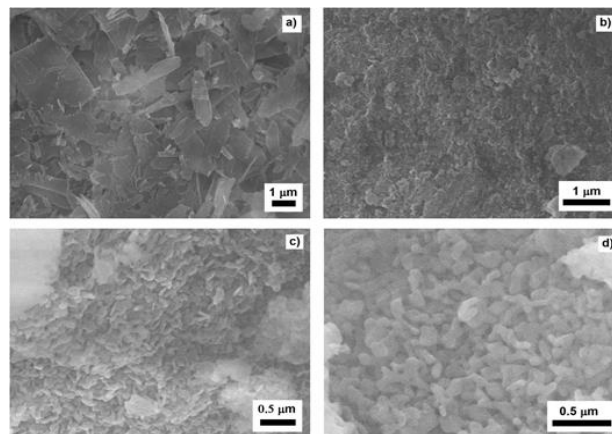
The starting materials for this synthesis were aluminum cans, glacial acetic acid, HCl, NaOH, and distilled water with a conductivity of $\sim 3 \mu\text{S}/\text{cm}$. Stoichiometric ratios are used to weigh and measure these ingredients. First, the aluminum can was cut to a size of $2 \times 2 \text{ cm}^2$, and glacial acetic acid was used to remove the paint and the inner covering polymer. Aluminum is dissolved in two ways: one uses HCl and the other uses acetic acid. In the first procedure, aluminum is dissolved into HCl, and NaOH is added dropwise to produce aluminum hydroxide. The precipitate was washed with distilled water until the electrical conductivity was below $50 \mu\text{S}/\text{cm}$ in residual water. Subsequently, the aluminum hydroxide precipitate was filtered, dried at 90°C, and treated in the temperature range of 900-1160°C. In the second procedure, aluminum is dissolved in glacial acetic acid for several days (90-150). Then, the white precipitate was centrifuged at 2500 RPM, washed, dried at 90°C, and treated in a temperature range of 900-1160°C [39].

Figure 28. XRD pattern of aluminum hydroxide and heat-treated powder at different temperatures for 3 hours (G = Gibbsite, Bh = Boehmite, and By = Bayerite) [39]



The crystal structure of the precursor and calcined powder was determined by XRD analysis. **Figure 28** shows the XRD pattern of aluminum hydroxide and the results of powder synthesis after being heat-treated by the HCl-NaOH route. The aluminum hydroxide precursor consists of a mixture of Gibbsite ($G = \text{Al}_2\text{O}_3 \cdot 3\text{H}_2\text{O}$), Boehmite ($\text{Bh} = \text{Al}_2\text{O}_3 \cdot \text{H}_2\text{O}$), and Bayerite ($\text{By} = \text{Al}_2\text{O}_3 \cdot 3\text{H}_2\text{O}$, a gibbsite polymorph). Only crystalline powder $\delta\text{-Al}_2\text{O}_3$ was obtained on the aluminum acetate route before reaching the $\alpha\text{-Al}_2\text{O}_3$ crystal phase, according to XRD patterns. The $\delta\text{-Al}_2\text{O}_3$ phase powder was obtained at 900°C using the NaCl-NaOH route, and a mixture of $\delta\text{-Al}_2\text{O}_3$ and $\theta\text{-Al}_2\text{O}_3$ phases was obtained at 1000°C . When the temperature was 1160°C , the $\alpha\text{-Al}_2\text{O}_3$ phase was formed. The

Figure 29. SEM images of precursors: (a) aluminum acetate, (b) aluminum hydroxide at 1100°C for 3 hours, (c) $\alpha\text{-Al}_2\text{O}_3$ from aluminum acetate, and (d) $\alpha\text{-Al}_2\text{O}_3$ from aluminum hydroxide [39]



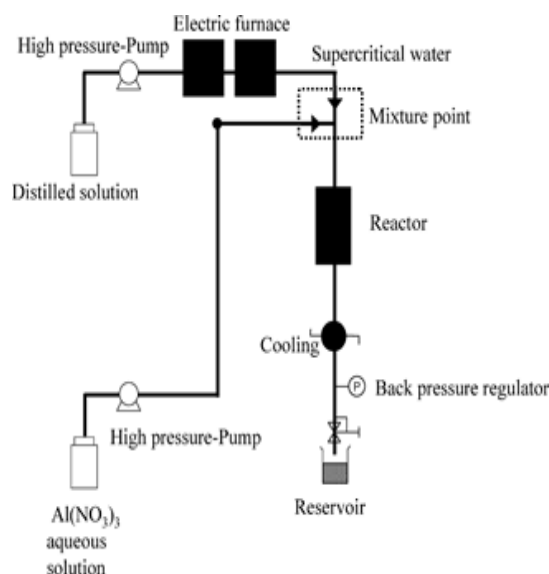
SEM image shown in **Figure 29** reveals the morphology of the untreated and heat-treated precursors at 1100°C of both procedures. As shown in **Figure 29c** and **Figure 29d**, the crystal sizes obtained from the aluminum acetate

and aluminum hydroxide samples after heat treatment at 1100°C were 54 nm and 58 nm, respectively [39]. This method is a little challenging to do because to dissolve AlCl_3 an acidic condition is needed to react with urea. Still, a relatively alkaline condition is needed when it has turned into $\gamma\text{-AlOOH}$ or AACH, with a pH value of 8.5-10. $\alpha\text{-Al}_2\text{O}_3$ obtained at a temperature of $1150\text{-}1100^\circ\text{C}$ is 20-30 nm in size [41].

3.5. Synthesis under supercritical water conditions method

The supercritical water method is one of the hydrothermal synthesis methods. To control the morphology of the material using low or high pressure is required depending on the composition of the reaction required. Using this method will reduce material losses [46]. The disadvantage of this method is that it results in agglomeration and large secondary particle size [42].

Figure 30. Schematic diagram of a flow reaction system [35]



Noguchi *et al.* [42] used a continuous flow system of chemicals using the supercritical water approach. Aluminum Nitrate ($\text{Al}(\text{NO}_3)_3 \cdot 9\text{H}_2\text{O}$ 99%) and 18 ohms distilled water are used in this procedure. The distilled water is placed in a container, then removed through a high-pressure hose with a flow rate of 24-43.5 g/min and a pressure of 25-35 MPa, entering an electric heater with a temperature of 585, while $\text{Al}(\text{NO}_3)_3$ is placed in a container and flowed through a high-pressure hose with a flow rate of 3.5-20 g/min and a pressure of 25-35 MPa. With hot distilled water, $\text{Al}(\text{NO}_3)_3$ will dissolve. A hydrothermal reaction occurs when the reactants enter the reactor tube at the correct temperature, producing $\gamma\text{-Al}_2\text{O}_3$ or AlOOH (**Figure 30**).

In the experiment, Noguchi *et al.* [35] is the first report for synthesizing γ -Al₂O₃ at a temperature of 410°C or the temperature in supercritical water. The results of γ -Al₂O₃ from γ -AlOOH become dominant due to the dehydration reaction resulting from a water density of 0.357-0.251 g/cm³ with a temperature of only 10°C. The size obtained is at 4-6 nm (Figure 31), depending on the temperature and reaction time. With increasing reagent concentration and decreasing pH, the particle size of γ -Al₂O₃ decreases. With increasing temperature and collection time, the particle size of γ -Al₂O₃ also increases.

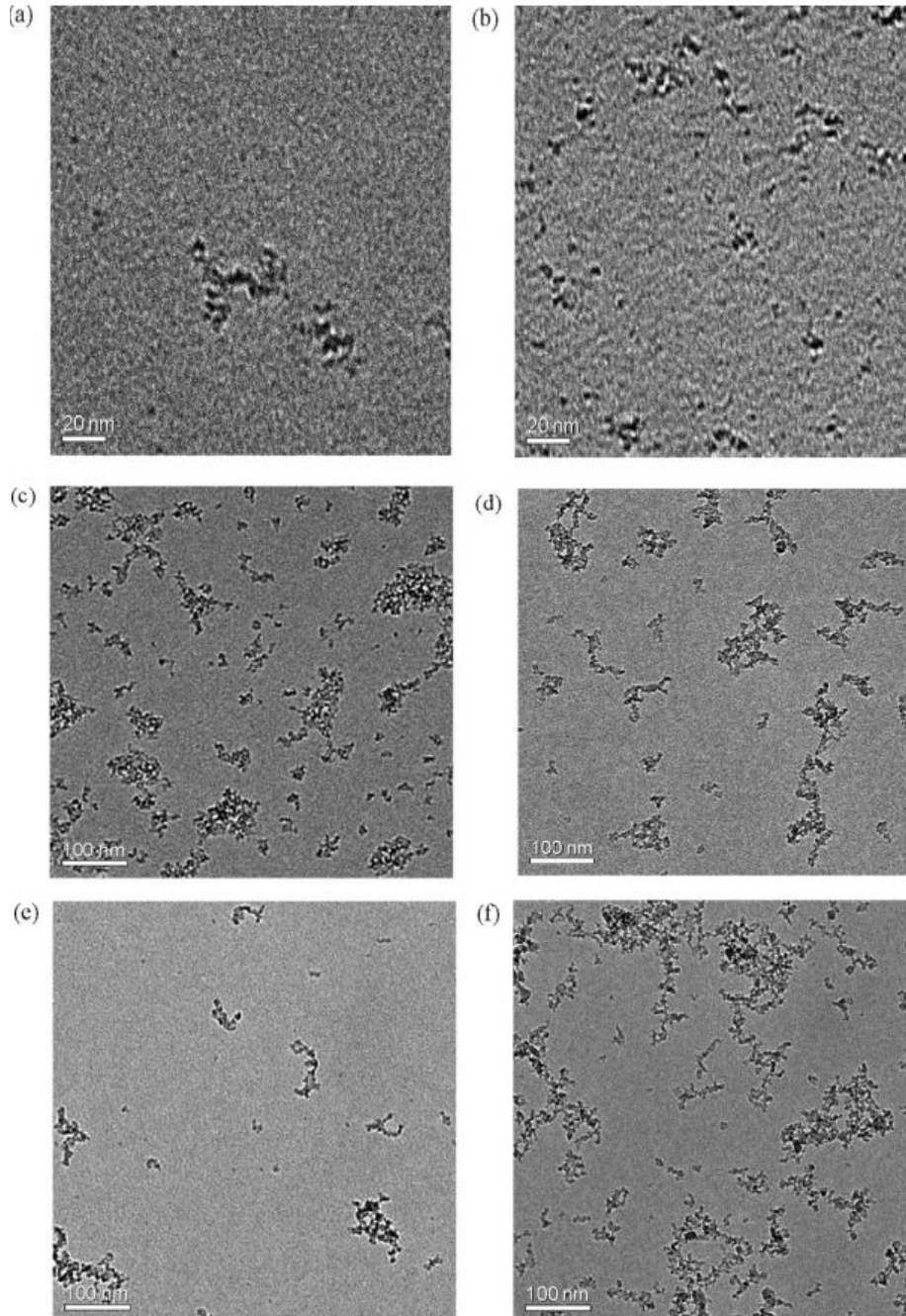


Figure 31. TEM image of γ -Al₂O₃ particles. Reaction pressure: 30 MPa, reaction temperature (°C)–Al(NO₃)₃·9H₂O concentration (M)–reaction time (s): (a) 425–0.1–0.12; (b) 425–0.3–0.12; (c) 425–0.1–1.2; (d) 450–0.1–3; (e) 500–0.1–2.6 and (f) 500–0.3–2.6. Image adapted from Noguchi *et al.* [35]

3.6. Microwave method

Microwave radiation can be used as a powerful heat source for the synthesis of nanoparticles from the liquid phase in a short time [43]. Microwave heating is considered a more efficient way of controlling heating because it requires less energy than conventional methods. This is due to the different heating mechanisms. In a microwave oven, the sample is generated within the sample itself due to the interaction of the microwaves with the material. Meanwhile, in conventional heating, the heat generated by the heating element is then transferred to the sample surface [50,51].

Hasanpoor *et al.* [43] synthesize Al_2O_3 nanoparticles using plant extracts by heating using a microwave. The materials used are Aluminum Nitrate (>98%), plant extracts, and ethanol. The plants used were *Syzygium aromaticum*, *Origanum vulgare*, *Origanum majorana*, *Theobroma cacao*, and *Cichorium intybus*. Aluminum nitrate (>98%) and plant extracts were mixed in a ratio of 1:4 by weight and then stirred. LG 850W microwave model No: MS1040SM/00v with a frequency of 2.45 GHz was used as the heat source and the solution was irradiated for 10 minutes at 610W. The irradiated solution was centrifuged and washed with ethanol and deionized water. The powder is dissolved in deionized water and treated with 150W ultrasonic vibration to reduce agglomeration.

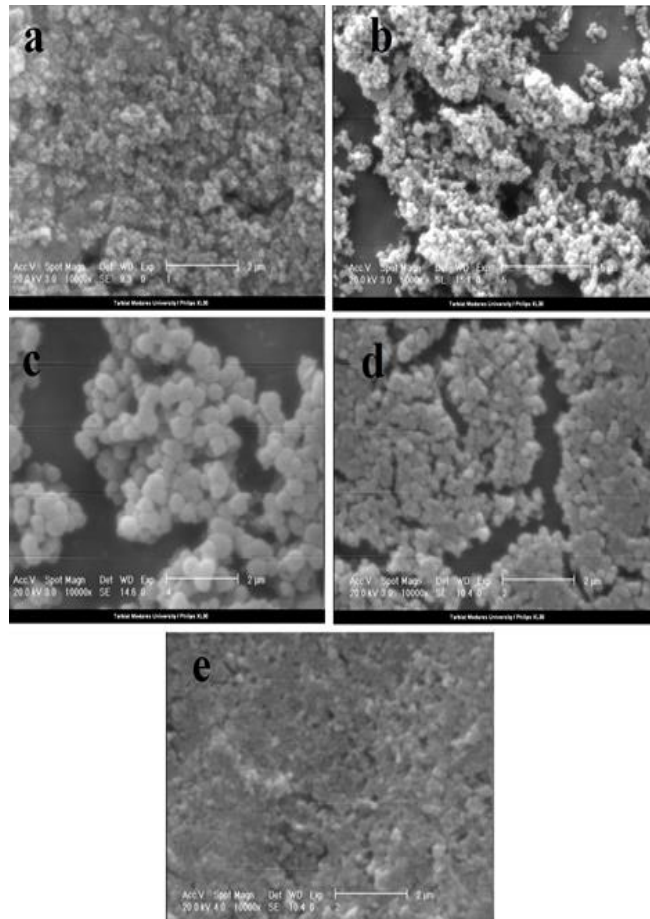


Figure 32.
SEM images of
(a) *Syzygium aromaticum*,
(b) *Origanum vulgare*,
(c) *Origanum majorana*,
(d) *Theobroma cacao*, and
(e) *Cichorium intybus* [43]

Hasanpoor *et al.* [43] reported the results of the synthesis showed that all the synthesized nanoparticles appeared to have an almost spherical shape. SEM analysis (Figure 29) shows a cluster of nanoparticles in the range of 60-300 nm. The nanoparticles are significantly smaller than the dimensions estimated from the SEM images, which could be due to nanoparticle aggregation. The XRD pattern (Figure 33) of the particles synthesized with *Syzygium aromaticum* showed a semi-crystalline structure while the others did not show significant peaks, possibly being in an amorphous structure. The nanoparticle size was less than 10 nm according to TEM and atomic force microscopy (AFM) studies, with average sizes of 8, 3, 5, 2, and 9 nm for *Syzygium aromaticum*, *Origanum vulgare*, *Origanum majorana*, *Theobroma cacao*, and *Cichorium intybus* plants, respectively.

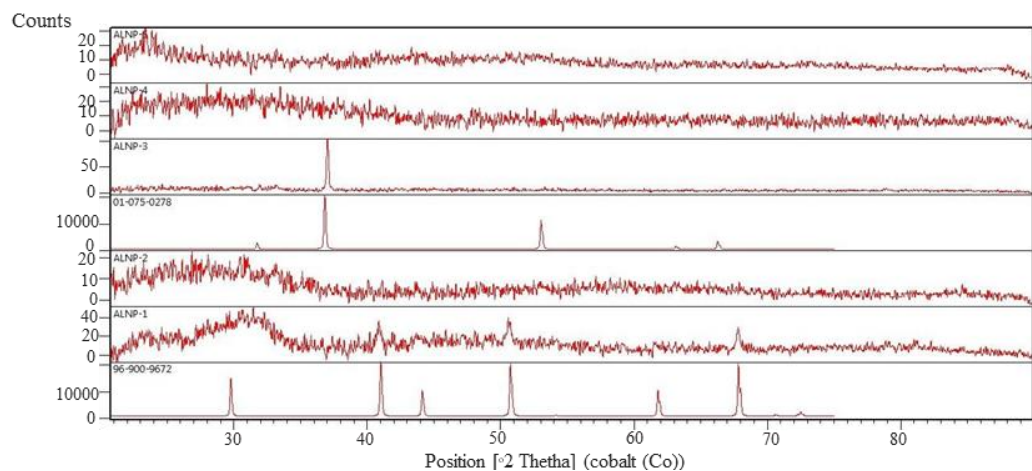


Figure 33.
XRD pattern of alumina
nanoparticles [43]

3.7. Mechanochemical method

The term "mechanochemical" refers to a chemical approach that employs the use of tools. The most common machine is ball milling, which grinds the powder to fine particle size and then mixes it with the mixture. The ground particles in this machine can be composed of glass [52]. Due to particle size reduction, intensive grinding increases the exterior contact area between reactant powders, allowing new surfaces to make contact [44]. Mechanochemical's advantages are useful for large-scale production, high purity, and cost-effective [53,54]. The disadvantages of mechanochemical are required high energy, long period of milling time, contamination of powder due steel balls, and susceptible microstructure can be grinded [55].

Gao *et al.* [41] reported on the mechanochemical production of α - Al_2O_3 . $\text{AlCl}_3 \cdot 6\text{H}_2\text{O}$ and NH_4HCO_3 , deionized water, and ammonium hydroxide were employed. The mixture of 0.03 moles of $\text{AlCl}_3 \cdot 6\text{H}_2\text{O}$ and 0.15 moles of NH_4HCO_3 is ground. After that, 20 mL of ammonium hydroxide solution (25%) was added and crushed. The pH of the final product will be 9-10. Deionized water and ethanol were used to filter and wash the precursors, respectively. Together with the precursor, the soluble starch was weighed and dispersed in anhydrous ethanol. After 30 minutes of sonication, the mixture was filtered and dried at 60°C for 30 minutes. The dry mixture was calcined for 1.5 hours at 1100°C in an air environment.

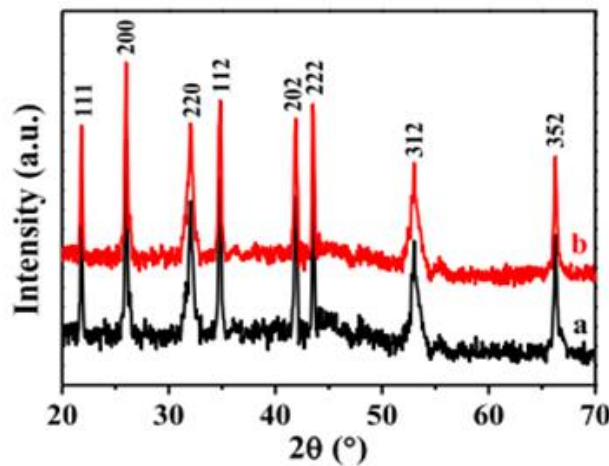


Figure 34. XRD pattern of sediment obtained from (a) wet-chemical and (b) mechanochemical methods [41]

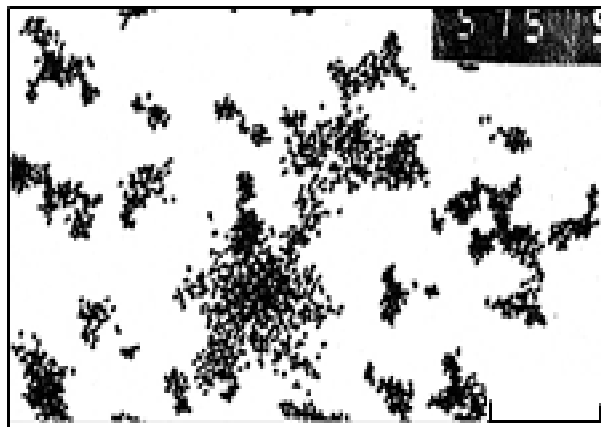


Figure 35. XRD pattern (a) TEM photograph of the α - Al_2O_3 powder prepared by the mechanochemical method [41]

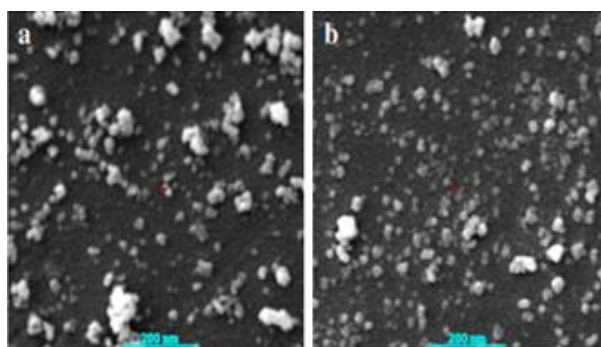


Figure 36. SEM display of α - Al_2O_3 powder prepared (a) without and (b) with starch as dispersant by the mechanochemical method [41]

In this method, the pH must be maintained to a value of 9-10 by adding ammonium hydroxide. Compared with the wet chemical method, this method is simpler, has lower calcination temperature, and results in fewer agglomerated nanoparticles, making it more suitable for commercial manufacture [41].

The results obtained by the research of Gao *et al.* [41] for this method, AACH is transformed into α - Al_2O_3 at a temperature of 1050 - 1100°C with a particle size of 30-40 nm. The XRD pattern of the mechanochemical is shown in Figure 34b. Figure 35 presented TEM photography of α - Al_2O_3 powder. Figure 36 is an SEM image of the α - Al_2O_3 powder prepared without and with starch as the dispersant.

The synthesis of α - Al_2O_3 by this approach was also published by Bodaghi *et al.* [37]. This mechanochemical approach, according to the literature, requires cheap manufacturing costs for big numbers. Fe_2O_3 and aluminum are the materials employed.

Bodaghi *et al.* [44] produced the results are α - Al_2O_3 crystals measuring 12-20 nm. Ball-milling yields nanocrystalline materials with amorphous fractions, and microstructures must be considered when employing these materials, according to the findings. In fact, the process's low temperature causes disruption, which leads to amorphization. Kinetics, rather than

thermodynamics, can dictate the final structure. XRD traces of iron (III) oxide and aluminum from 1 to 100 hours are shown in Figure 37. Figure 38 presented SEM micrographs of milled particles over time. The TEM sizes are shown in Figure 39 and Figure 40 under various settings. Figure 41 depicts the high-resolution transmission electron microscopy (HR-TEM) of the powder mixture after 20 hours.

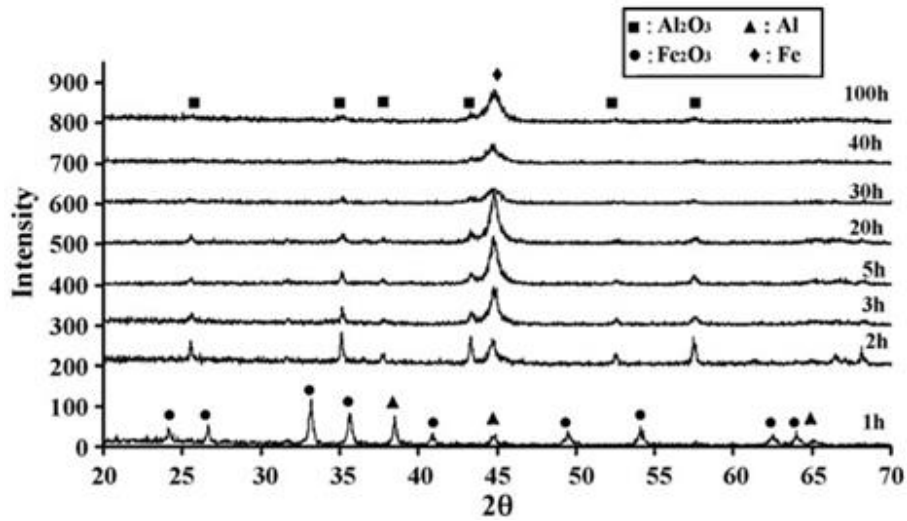


Figure 37. XRD pattern of the sample for $t=1-100$ h [44]

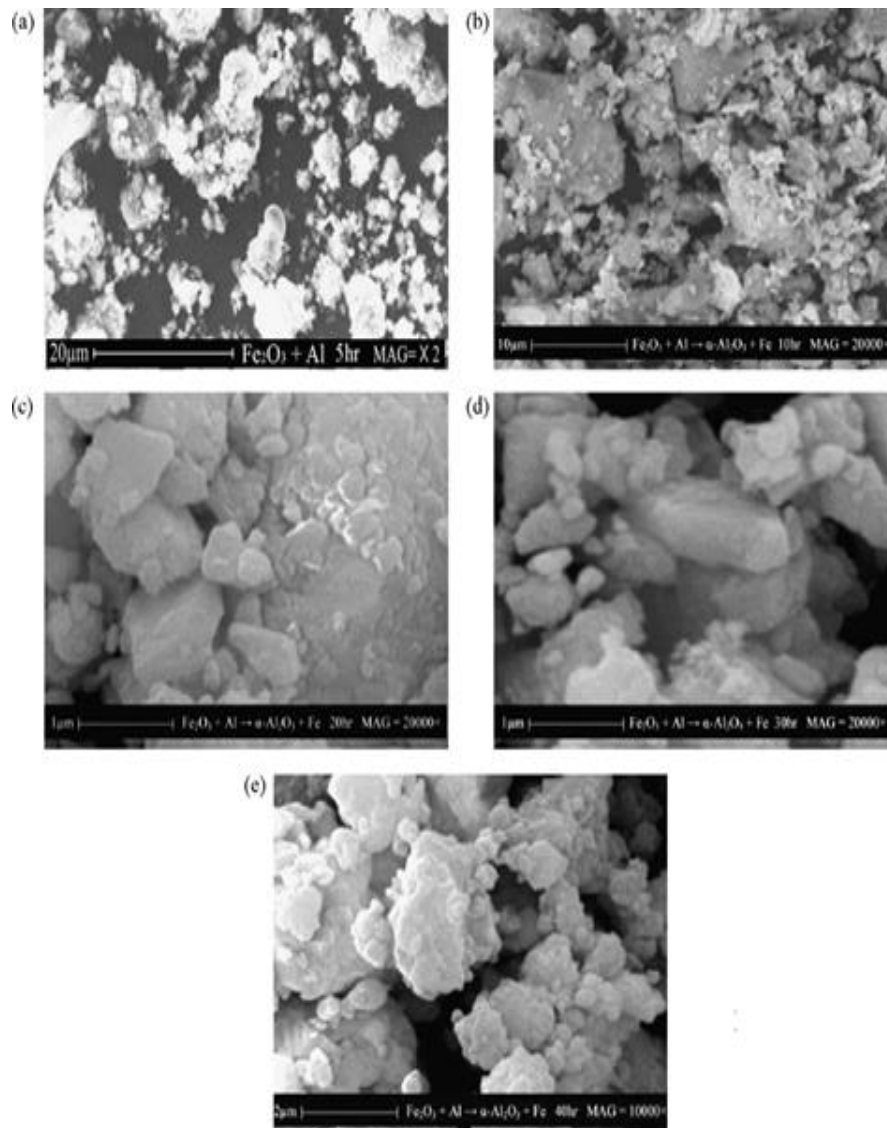


Figure 38. SEM micrograph (second electron mode) of $\alpha\text{-Al}_2\text{O}_3$ nanocrystal formed from the reduction of hematite under mechanical alloying for (a) 5h, (b) 10 h, (c) 20 h, (d) 30 h, and (e) 40 h [44]

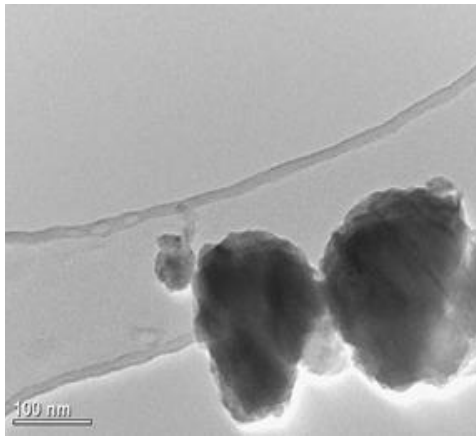


Figure 39.
TEM image of the powder mixture ground for 20 hours before washing with HCl [44]

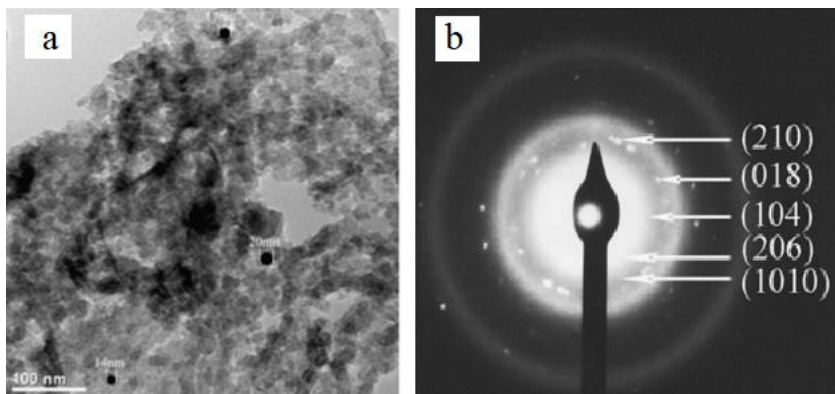


Figure 40.
TEM image of a powder mixture ground for 20 h after 20 h with HCl (α - Al_2O_3) (a) bright-field TEM micrograph (b) SADP association [44]

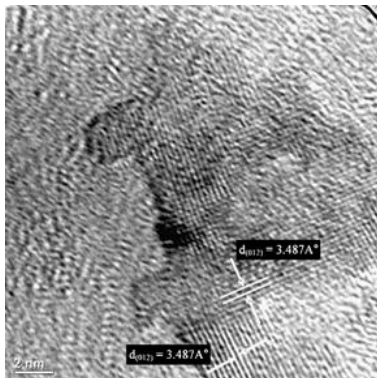


Figure 41.
HR-TEM image of the powder mixture for 20 h after washing with HCl [44]

3.8. Hydrolysis method

One of the methods for synthesizing Al_2O_3 nanoparticles is hydrolysis, which is based on the hydrolysis reaction of the raw materials mixed in the reactor and depends on temperature. This method yields nanoparticles with a large surface area and high thermal stability [45].

This synthesis uses aluminum phosphide powder (>85%) and deionized water as the starting material. These ingredients are weighed and measured in stoichiometric ratios. First, deionized water is added to the aluminum phosphide powder in the reactor. The temperature of the reaction was kept constant at 363 K. After the reaction was completed and cooled to room temperature, a precipitate of aluminum hydroxide was obtained and filtered, and washed with deionized water. The PAIOH sample was prepared by drying the filter cake at 373 K for 12 hours, and the PAI-773 sample was prepared by calcining the PAIOH at 773 K for 3 hours [45].

The XRD results of the PAIOH samples calcined at different temperatures are shown in Figure 42. The diffraction pattern of bayerite disappeared after calcination at 773 K. Weak peaks of γ - Al_2O_3 , and different AlN peaks were observed. The phase, degree of crystallinity, and crystal size all influence the XRD peak intensity. Perfect crystals and large crystal dimensions lead to high intensity of characteristic peaks. The intensity of the diffraction peak increases as the calcination temperature rises, and more other phases appear. The crystallites grew with fewer defects after being calcined at 1273 K, as evidenced by the increase in the peak intensity of the γ - Al_2O_3 phase.

The γ - Al_2O_3 and θ - Al_2O_3 phases predominated after 3 hours of calcination at 1473 K, with a minor α - Al_2O_3 phase. Figure 43 reveals the morphological change from needle-like to rod-like after calcination at 1473 K. These nano bars were irregular in shape, with a diameter of 7-8 nm and a length of 130 nm [45].

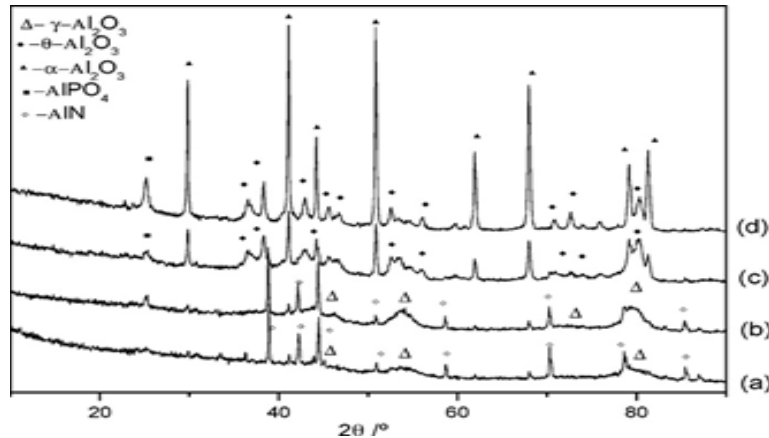


Figure 42. XRD pattern of synthesized PAI calcined for 3 hours at (a) 773 K, (b) 1273 K, (c) 1473 K, and (d) 1573 K [45]

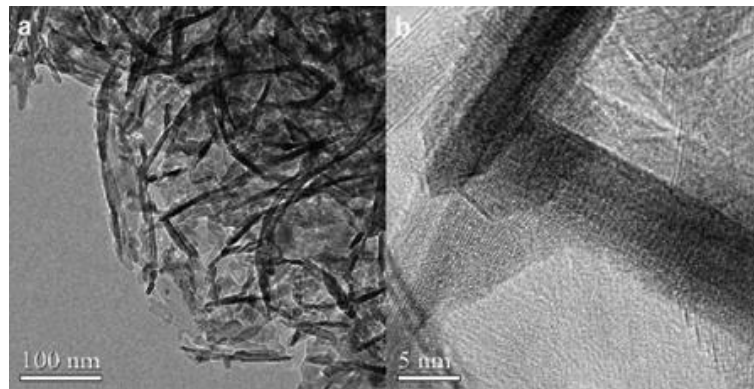


Figure 43. TEM electron micrograph of calcined PAI synthesized powder at 1473 K. (a) low magnification image and (b) high magnification image [45]

4. Conclusion

Several methods can be used to synthesize Al_2O_3 , such as (1) precipitation, (2) combustion, (3) sol-gel, (4) wet chemical, (5) synthesis in supercritical water conditions, (6) microwave, (7) mechanochemical, and (8) hydrolysis. Precipitation is the most efficient method for synthesizing Al_2O_3 . It is the simplest compared to other methods, has low raw material costs, produces no pollution, and has several advantages such as high purity products, nearly homogeneous nanoparticles in size, excellent thermal conductivity, and controlling desired particle size. Further research is needed to determine the most effective materials and efficient procedure in using the precipitation method.

Acknowledgment

We acknowledged Bangdos Universitas Pendidikan Indonesia.

Authors' Declaration

This research was supported by:



Authors' contributions and responsibilities - The authors made substantial contributions to the conception and design of the study. The authors took responsibility for data analysis, interpretation, and discussion of results. The authors read and approved the final manuscript.

Funding - No specific funding statement from the authors

Availability of data and materials - All data are available from the authors.

Competing interests - The authors declare no competing interest.

Additional information - No additional information from the authors

References

- [1] P. A. Prashanth et al., "Synthesis, characterizations, antibacterial and photoluminescence studies of solution combustion-derived α -Al₂O₃ nanoparticles," *Journal Asian Ceramic Society*, vol. 3, no. 3, pp. 345–351, 2015, doi: 10.1016/j.jascer.2015.07.001.
- [2] M. S. Y. Parast and A. Morsali, "Synthesis and characterization of porous Al(III) metal-organic framework nanoparticles as a new precursor for preparation of Al₂O₃ Nanoparticles," *Inorganic Chemistry Community*, vol. 14, no. 5, pp. 645–648, 2011, doi: 10.1016/j.inoche.2011.01.040.
- [3] L. Zhu et al., "Low temperature synthesis of polyhedral α -Al₂O₃ nanoparticles through two different modes of planetary ball milling," *Ceramic International*, vol. 46, no. 18, pp. 28414–28421, 2020, doi: 10.1016/j.ceramint.2020.07.346.
- [4] Simón Y. Reyes López, Juan Serrato Rodríguez, Satoshi Sugita Sueyoshi, "Low-temperature formation of alpha alumina powders via metal organic synthesis," *The AZo Journal of Materials Online*, vol. 2, no. April, pp. 1–9, 2006.
- [5] M. T. Hernández and M. González, "Synthesis of resins by microwave and infrared heating as precursors of alpha-alumina. Comparison of the results," *Key Engineering Materials*, vol. 206–213, no. 1, pp. 71–74, 2001, doi: 10.4028/www.scientific.net/kem.206-213.71.
- [6] K. Laishram, R. Mann, and N. Malhan, "A novel microwave combustion approach for single step synthesis of α -Al₂O₃ nanopowders," *Ceramic International*, vol. 38, no. 2, pp. 1703–1706, 2012, doi: 10.1016/j.ceramint.2011.08.044.
- [7] H. Gao, M. Zhang, H. Yang, Z. Li, Y. Li, and L. Chen, "A novel green synthesis of γ -Al₂O₃ nanoparticles using soluble starch," *Modern Physics Letter. B*, vol. 33, no. 16, pp. 1–9, 2019, doi: 10.1142/S0217984919501823.
- [8] G. W. Lee, "Phase Transition Characteristics of with Heat Treatment," *International Journal Chemical Nuclear Metallurgy Materials*, vol. 7, no. 9, pp. 699–702, 2013.
- [9] A. Rajaeiyan and M. M. Bagheri-Mohagheghi, "Comparison of sol-gel and co-precipitation methods on the structural properties and phase transformation of γ and α -Al₂O₃ nanoparticles," *Advance in Manufacturing*, vol. 1, no. 2, pp. 176–182, 2013, doi: 10.1007/s40436-013-0018-1.
- [10] L. Song, Y. Dong, Q. Shao, and J. Jiang, "Synthesis of monodisperse α -Al₂O₃ nanoparticles by a salt microemulsion method," *Micro Nano Letter*, vol. 13, no. 8, pp. 1071–1074, 2018, doi: 10.1049/mnl.2018.0078.
- [11] S. N. S. Mohamad, N. Mahmed, D. S. Che Halin, K. Abdul Razak, M. N. Norizan, and I. S. Mohamad, "Synthesis of alumina nanoparticles by sol-gel method and their applications in the removal of copper ions (Cu²⁺) from the solution," *IOP Conference Series: Material Science Engineering*, vol. 701, no. 1, 2019, doi: 10.1088/1757-899X/701/1/012034.
- [12] A. A. Mohammed, Z. T. Khodair, and A. A. Khadom, "Preparation and investigation of the structural properties of α -Al₂O₃ nanoparticles using the sol-gel method," *Chemical Data Collection*, vol. 29, p. 100531, 2020, doi: 10.1016/j.cdc.2020.100531.
- [13] H. S. Potdar, K. W. Jun, J. W. Bae, S. M. Kim, and Y. J. Lee, "Synthesis of nano-sized porous γ -alumina powder via a precipitation/digestion route," *Applied Catalysis A: General*, vol. 321, no. 2, pp. 109–116, 2007, doi: 10.1016/j.apcata.2007.01.055.
- [14] S. Wang, X. Li, S. Wang, Y. Li, and Y. Zhai, "Synthesis of γ -alumina via precipitation in ethanol," *Material Letter*, vol. 62, no. 20, pp. 3552–3554, 2008, doi: 10.1016/j.matlet.2008.03.048.
- [15] X. Su, S. Chen, and Z. Zhou, "Synthesis and characterization of monodisperse porous α -Al₂O₃ nanoparticles," *Applied Surface Science*, vol. 258, no. 15, pp. 5712–5715, 2012, doi: 10.1016/j.apsusc.2012.02.067.

- [16] S. A. Hassanzadeh-Tabrizi and E. Taheri-Nassaj, "Economical synthesis of Al₂O₃ nanopowder using a precipitation method," *Material Letter* vol. 63, no. 27, pp. 2274–2276, 2009, doi: 10.1016/j.matlet.2009.07.035.
- [17] A. S. Jbara, Z. Othaman, A. A. Ati, and M. A. Saeed, "Characterization of γ -Al₂O₃ nanopowders synthesized by Co-precipitation method," *Materials Chemistry and Physics*, vol. 188, pp. 24–29, 2017, doi: 10.1016/j.matchemphys.2016.12.015.
- [18] Y. S. Wu, J. Ma, F. Hu, and M. C. Li, "Synthesis and characterization of mesoporous alumina via a reverse precipitation method," *Journal of Materials Science & Technology*, vol. 28, no. 6, pp. 572–576, 2012, doi: 10.1016/S1005-0302(12)60100-5.
- [19] Wang, J., Zhao, D., Zhou, G., Zhang, C., Zhang, P., & Hou, X. (2020). Synthesis of nano-sized γ -Al₂O₃ with controllable size by simple homogeneous precipitation method. *Materials Letters*, 128476. doi:10.1016/j.matlet.2020.128476
- [20] W. Wang, K. Zhang, Y. Yang, H. Liu, Z. Qiao, and H. Luo, "Synthesis of mesoporous Al₂O₃ with large surface area and large pore diameter by improved precipitation method," *Microporous Mesoporous Mater.*, vol. 193, pp. 47–53, 2014, doi: 10.1016/j.micromeso.2014.03.008.
- [21] J. Kong, B. Chao, T. Wang, and Y. Yan, "Preparation of ultrafine spherical AlOOH and Al₂O₃ powders by aqueous precipitation method with mixed surfactants," *Powder Technology*, vol. 229, pp. 7–16, 2012, doi: 10.1016/j.powtec.2012.05.024.
- [22] K. M. Parida, A. C. Pradhan, J. Das, and N. Sahu, "Synthesis and characterization of nano-sized porous gamma-alumina by control precipitation method," *Materials Chemistry and Physics*, vol. 113, no. 1, pp. 244–248, 2009, doi: 10.1016/j.matchemphys.2008.07.076.
- [23] J. Hong Yi, Y. Yi Sun, J. Feng Gao, and C. Yan Xu, "Synthesis of crystalline γ -Al₂O₃ with high purity," *Trans. Nonferrous Metal Society China (English Ed.)*, vol. 19, no. 5, pp. 1237–1242, 2009, doi: 10.1016/S1003-6326(08)60435-5.
- [24] H. Li, H. Lu, S. Wang, J. Jia, H. Sun, and X. Hu, "Preparation of a nano-sized α -Al₂O₃ powder from a supersaturated sodium aluminate solution," *Ceramics International*, vol. 35, no. 2, pp. 901–904, 2009, doi: 10.1016/j.ceramint.2008.01.030.
- [25] S. Ali, Y. Abbas, Z. Zuhra, and I. S. Butler, "Synthesis of γ -alumina (Al₂O₃) nanoparticles and their potential for use as an adsorbent in the removal of methylene blue dye from industrial wastewater," *Nanoscale Advance*, vol. 1, no. 1, pp. 213–218, 2019, doi: 10.1039/c8na00014j.
- [26] M. Farahmandjou and N. Golabiyan, "Synthesis and characterisation of Al₂O₃ nanoparticles as catalyst prepared by polymer co-precipitation method," *Material Engineering Research*, vol. 1, no. 2, pp. 40–44, 2019, doi: 10.25082/mer.2019.02.002.
- [27] V. V. Karasev et al., "Formation of charged aggregates of Al₂O₃ nanoparticles by combustion of aluminum droplets in air," *Combustion and Flame*, vol. 138, no. 1–2, pp. 40–54, Jul. 2004, doi: 10.1016/j.combustflame.2004.04.001.
- [28] D. G. Syarif, M. Yamin, and Y. I. Pratiwi, "Self combustion synthesis of Al₂O₃ nanoparticles from bauxite utilizing sugar as fuel for nanofluids with enhanced CHF," *Journal of Physics: Conference Series*, vol. 1153, no. 1, 2019, doi: 10.1088/1742-6596/1153/1/012068.
- [29] F. B. Afruz and M. J. Tafreshi, "Synthesis of γ -Al₂O₃ nano particles by different combustion modes using ammonium carbonate," *Indian Journal Pure and Applied Physical*, vol. 52, no. 6, pp. 378–385, 2014.
- [30] Z. Hosseini, M. Taghizadeh, and F. Yaripour, "Synthesis of nanocrystalline γ -Al₂O₃ by sol-gel and precipitation methods for methanol dehydration to dimethyl ether," *Journal of Natural Gas Chemistry*, vol. 20, no. 2, pp. 128–134, 2011, doi: 10.1016/S1003-9953(10)60172-7.
- [31] J. Li, Y. Pan, C. Xiang, Q. Ge, and J. Guo, "Low temperature synthesis of ultrafine α -Al₂O₃ powder by a simple aqueous sol-gel process," *Ceramics International*, vol. 32, no. 5, pp. 587–591, 2006, doi: 10.1016/j.ceramint.2005.04.015.

- [32] S. M. Kim, Y. J. Lee, K. W. Jun, J. Y. Park, and H. S. Potdar, "Synthesis of thermo-stable high surface area alumina powder from sol-gel derived boehmite," *Materials Chemistry and Physics*, vol. 104, no. 1, pp. 56–61, 2007, doi: 10.1016/j.matchemphys.2007.02.044.
- [33] M. Shojaie-Bahaabad and E. Taheri-Nassaj, "Economical synthesis of nano alumina powder using an aqueous sol-gel method," *Materials Letters*, vol. 62, no. 19, pp. 3364–3366, 2008, doi: 10.1016/j.matlet.2008.03.012.
- [34] S. Dubey, A. Singh, B. Nim, and I. B. Singh, "Optimization of molar concentration of AlCl_3 salt in the sol-gel synthesis of nanoparticles of gamma alumina and their application in the removal of fluoride of water," *Journal of Sol-Gel Science and Technology*, vol. 82, no. 2, pp. 468–477, 2017, doi: 10.1007/s10971-017-4336-9.
- [35] P. Nayar, S. Waghmare, P. Singh, M. Najar, S. Puttewar, and A. Agnihotri, "Comparative study of phase transformation of Al_2O_3 nanoparticles prepared by chemical precipitation and sol-gel auto combustion methods," *Material Today Proceedings*, vol. 26, no. xxxx, pp. 122–125, 2018, doi: 10.1016/j.matpr.2019.05.450.
- [36] O. M. Rosadi, " Al_2O_3 nanoparticles synthesis using sol-gel process to improve cooling engine performance," *eProceedings of Engineering*, vol. 3, no. 1, pp. 622–627, 2016, [Online]. Available: <https://openlibrary.telkomuniversity.ac.id/home/catalog/id/114808/slug/al2o3-nanoparticles-synthesis-using-sol-gel-process-to-improve-cooling-engine-performance.html> (accessed July 05, 2021).
- [37] V. Pandurang Dhawale, "Synthesis and characterization of aluminium oxide (Al_2O_3) nanoparticles and its application in azodye decolourisation," *International Journal Environmental Chemistry*, vol. 2, no. 1, p. 10, 2018, doi: 10.11648/j.ijec.20180201.13.
- [38] H. Lu, H. Sun, A. Mao, H. Yang, H. Wang, and X. Hu, "Preparation of plate-like nano $\alpha\text{-Al}_2\text{O}_3$ using nano-aluminum seeds by wet-chemical methods," *Material Science Engineering A*, vol. 406, no. 1–2, pp. 19–23, 2005, doi: 10.1016/j.msea.2005.04.047.
- [39] R. López-Juárez, N. Razo-Perez, T. Pérez-Juache, O. Hernandez-Cristobal, and S. Y. Reyes-López, "Synthesis of $\alpha\text{-Al}_2\text{O}_3$ from aluminum cans by wet-chemical methods," *Results in Physics*, vol. 11, no. November, pp. 1075–1079, 2018, doi: 10.1016/j.rinp.2018.11.037.
- [40] H. X. Lu, J. Hu, C. P. Chen, H. W. Sun, X. Hu, and D. L. Yang, "Characterization of $\text{Al}_2\text{O}_3\text{-Al}$ nano-composite powder prepared by a wet chemical method," *Ceramics International*, vol. 31, no. 3, pp. 481–485, 2005, doi: 10.1016/j.ceramint.2004.06.014.
- [41] H. Gao, Z. Li, and P. Zhao, "Green synthesis of nanocrystalline $\alpha\text{-Al}_2\text{O}_3$ powders by both wet-chemical and mechanochemical methods," *Modern Physics Letters B*, vol. 32, no. 8, pp. 1–9, 2018, doi: 10.1142/S0217984918501099.
- [42] T. Noguchi, K. Matsui, N. M. Islam, Y. Hakuta, and H. Hayashi, "Rapid synthesis of $\gamma\text{-Al}_2\text{O}_3$ nanoparticles in supercritical water by continuous hydrothermal flow reaction system," *Journal of Supercritical Fluids*, vol. 46, no. 2, pp. 129–136, 2008, doi: 10.1016/j.supflu.2008.04.011.
- [43] M. Hasanpoor, H. Fakhr Nabavi, and M. Aliofkhazraei, "Microwave-assisted synthesis of alumina nanoparticles using some plants extracts," *Journal of Nanostructures*, vol. 7, no. 1, pp. 40–46, 2017, doi: 10.22052/jns.2017.01.005.
- [44] M. Bodaghi, A. Mirhabibi, M. Tahriri, H. Zolfonoon, and M. Karimi, "Mechanochemical assisted synthesis and powder characteristics of nanostructure ceramic of $\alpha\text{-Al}_2\text{O}_3$ at room temperature," *Materials Science and Engineering B: Solid-State Materials for Advanced Technology*, vol. 162, no. 3, pp. 155–161, 2009, doi: 10.1016/j.mseb.2009.03.021.
- [45] Y. Wang, J. Wang, M. Shen, and W. Wang, "Synthesis and properties of thermostable γ -alumina prepared by hydrolysis of phosphide aluminum," *Journal of Alloys and Compounds*, vol. 467, no. 1–2, pp. 405–412, 2009, doi: 10.1016/j.jallcom.2007.12.007.
- [46] A. Varma, A. S. Mukasyan, A. S. Rogachev, and K. V. Manukyan, "Solution combustion synthesis of nanoscale materials," *Chemical Reviews*, vol. 116, no. 23, pp. 14493–14586, 2016, doi: 10.1021/acs.chemrev.6b00279.

- [47] M. I. Kandil, H. S. Jahin, H. A. Dessouki, and M. Y. Nassar, "Synthesis and characterization of γ -Al₂O₃ and α -Al₂O₃ nanoparticles using a facile, inexpensive auto-combustion approach," *Egypt. J. Chem.*, vol. 64, no. 5, pp. 2509–2515, 2021, doi: 10.21608/EJCHEM.2021.61793.3330
- [48] R. Rogojan, E. Andronescu, C. Ghițuică, and B. Ștefan Vasile, "Synthesis and characterization of alumina nano-powder obtained by sol-gel method," *UPB Scientific Bulletin Series B Chemical Material Science*, vol. 73, no. 2, pp. 67–76, 2011.
- [49] Y. X. Gan, A. H. Jayatissa, Z. Yu, X. Chen, and M. Li, "Hydrothermal synthesis of nanomaterials," *Journal of Nanomaterials.*, vol. 2020, 2020, doi: 10.1155/2020/8917013.
- [50] A. Kumar, Y. Kuang, Z. Liang, and X. Sun, "Microwave chemistry, recent advancements, and eco-friendly microwave-assisted synthesis of nanoarchitectures and their applications: a review," *Material Today Nano*, vol. 11, p. 100076, 2020, doi: 10.1016/j.mtnano.2020.100076.
- [51] L. Sharifi, M. Beyhaghi, T. Ebadzadeh, and E. Ghasemi, "Microwave-assisted sol-gel synthesis of alpha alumina nanopowder and study of the rheological behavior," *Ceramic International*, vol. 39, no. 2, pp. 1227–1232, 2013, doi: 10.1016/j.ceramint.2012.07.050.
- [52] A. T. Simbara, A. L. Muharam, I. Hanifa, K. M. Rizky, R. F. Fadhillah, and A. B. D. Nandiyanto, "Review: comparison of the LiBH₄ material synthesis method and its application as hydrogen energy storage," *Journal of Applied Science and Environmental Studies*, vol. 3, no. 4, pp. 232–253, 2020.
- [53] M. Ullah, M. E. Ali, and S. B. A. Hamid, "Surfactant-assisted ball milling: A novel route to novel materials with controlled nanostructure-A review," *Reviews Advanced Material Sciences*, vol. 37, no. 1–2, pp. 1–14, 2014
- [54] A. Mohapatra, S. Agarwal, and M. Genesereth, "Policies," *Lecture Notes in Computer Science (including subseries Lecture Notes in Artificial Intelligence and Lecture Notes in Bioinformatics)*, vol. 9992 LNAI, pp. 291–302, 2016, doi: 10.1007/978-3-319-50127-7_24.
- [55] S. Thamizharasan and N. A. Saravanan, "Nanosization of drug biomaterials and its solubility enhancement by high energy ball milling," *Journal Nanoscience Technology*, vol. 5, no. 1, pp. 237–239, 2017, [Online]. Available: <http://jacsdirectory.com/journal-of-nanoscience-and-technology/articleview.php?id=67> (accessed July 05, 2021).